IEEE Access
Multidisciplinary : Rapid Review : Open Access Journal

Received 25 June 2024, accepted 11 July 2024, date of publication 15 July 2024, date of current version 23 July 2024.

Digital Object Identifier 10.1109/ACCESS.2024.3428328

RESEARCH ARTICLE

Enhancing Power System Performance via TCSC Technology Allocation With Enhanced Gradient-Based Optimization Algorithm

ALI S. ALJUMAH[1], MOHAMMED H. ALQAHTANI[1], (Member, IEEE), ABDULLAH M. SHAHEEN[2], AND ABDALLAH M. ELSAYED[3]

[1]Department of Electrical Engineering, College of Engineering, Prince Sattam Bin Abdulaziz University, Al-Kharj 16278, Saudi Arabia
[2]Department of Electrical Engineering, Faculty of Engineering, Suez University, Suez 43221, Egypt
[3]Electrical Engineering Department, Faculty of Engineering, Damietta University, Damietta 34517, Egypt

Corresponding authors: Ali S. Aljumah (as.aljumah@psau.edu.sa) and Abdullah M. Shaheen (abdullah.mohamed.eng19@suezuni.edu.eg)

This work was supported by Prince Sattam Bin Abdulaziz University under Project PSAU/2024/01/29312.

ABSTRACT This paper addresses the critical challenge of optimal allocation of Thyristor-Controlled Series Compensator (TCSC) devices in transmission power systems through an innovative optimization framework. Leveraging an Enhanced Gradient-Based Algorithm (EGBA) augmented with a crossover operator, the proposed methodology seeks to promote diversity in the solutions generated in each iteration, aiming to maximize the efficiency of power transmission networks. The algorithm incorporates key components such as the Gradient Search Process (GSP) and Local Escaping Process (LEP) to guide the exploration process and prevent premature convergence to suboptimal solutions. Additionally, the crossover operator, a novel addition in the EGBA, facilitates the exchange of TCSC configurations between solutions, contributing to solution diversity and potentially revealing novel optimal allocations. Initially, the EGBA and GBA performances are estimated using the CEC 2017 benchmarks. Moreover, to assess the practical applicability of the suggested EGBA, it is specifically tailored and implemented to enhance the operation of transmission power systems. The primary objective is to minimize technical power losses, considering varying numbers of TCSC devices with experimentation on two distinct IEEE power systems, one with 30 buses and another with 57 buses. The results are analyzed to validate the ability of the EGBA method in optimizing power systems and addressing technical losses. The novel proposed EGBA method significantly reduces power losses compared to the original GBA method in both tested power systems. In the first system, the EGBA achieved 0.85%, 2.99%, and 1.32% lower losses than the GBA when optimizing for one, two, and three TCSC devices, respectively. In addition, the objective of enhancing the security margin of the transmission lines is involved to optimize the power flow besides the minimization function of power losses. Similarly, in the second system, the EGBA outperformed the original GBA by 5.19%, 6.32%, and 5.12% for the same TCSC configurations. The simulation results demonstrate that the proposed EGBA is not only more effective but also more efficient than the original GBA and other recent approaches.

INDEX TERMS TCSC technology, TCSC allocation optimization, gradient-based algorithm, CEC 2017 benchmarks, transmission systems.

I. INTRODUCTION

A static non-linear programming issue that takes into consideration the electrical elements of massive transmission power grids is called the optimal power flow (OPF). While

The associate editor coordinating the review of this manuscript and approving it for publication was Rossano Musca.

optimizing vital objectives, the primary purpose of the challenge is to identify the steady-state functioning points of all electric elements accessible to the power systems [1], [2]. The OPF problem takes into account several individual goals, including entire power losses, the fuel costs for power generation electricity, voltage deviations, polluted emissions, and voltage stability index [3]. Furthermore, the issue of OPF requires that a set of operational and physical constraints be accurately met. These constraints include those enforced by devices and network limitations, such as switchable capacitor banks, transmission line capacity limits, bus voltages, transformer taps, active and reactive generators' power, and transformer taps [4], [5]. Essentially, in order to obtain other dependent variables such as the voltage magnitude at other buses, and the reactive power of the generators, the control variables such as voltage magnitude at generation buses, the active power of the generators, transformer tap settings, and injected reactive power at capacitor buses of the OPF problem must first be determined [6], [7], [8].

Real-world electrical networks frequently use TCSC technology due to the fact that is a robust and reasonably priced series FACTs device with exceptional performance that enables precise, dependable power flow regulation of power lines [9]. The use of TCSC devices, which provide series compensating characteristics, is one of the most affordable approaches to increase the transmission network's real electrical carrying capacity [10], [11]. In order to reduce area frequency fluctuations and tie-line power, three series FACTs apparatuses, which are the thyristor controlled phase shifter (TCPS), the TCSC, and the static synchronous series compensator (SSSC), are being considered and emulated in Automatic Generation Control (AGC) assessments pertaining to multi-area associated electrical networks [12]. The Improved Particle Swarm Optimization Technique (IPSOT) has been employed as a solution tool in conjunction with the Integral of Time multi-plied Squared Error (ITSE) as the goal of reduction to construct the damper controllers. In terms of vibration dampening at area frequencies and tie-line transmission powers, the TCSC-AGC has demonstrated better performance than the TCPS and SSSC. Sensitivity testing has also been conducted to demonstrate the TCSC-AGC's resilience through the practical deployment of the TCSC in transmission networks that highlighted its benefits over SSSC [13]. A variety of conventional and metaheuristic methods have recently been developed to address OPF such as sequential unconstrained methodology [14], interior point method [15], fuzzy linear framework [16], linear and nonlinear programming [17], [18], and Newton-based method [19] are examples of conventional methodologies. It should be highlighted, therefore, that these techniques are not helpful for significant electrical networks and do not result in globally optimum solutions. Thus, scientists have worked to develop metaheuristic techniques to overcome the shortcomings of earlier approaches [20].

Consequently, developing metaheuristic techniques is essential to overcoming the above-described limitations. Using a range of heuristic (population-based) approaches to tackle different OPF challenges has been more common in the last 20 years [21], [22]. Various solutions for augmenting the procedures have been characterized to reduce the power losses. An improved social spider optimizer has been outlined in [23] that balances the movement patterns of male and female spiders to minimize power losses. An alteration was made to the JAYA algorithm, enhancing its capability to refine generated solutions by incorporating adjustments based on the worst and best solutions regarding voltage profile and losses [24]. Gorilla troops optimizer was developed for designing fractional order controller integrating tilt integral derivative for stabilizing a three-area hybrid power system in [25] while a grasshopper optimization was hybridized with bald eagle searching algorithm [26] to address the unit commitment. In [27], graphical processing units (GPU-native sparse direct solver) have been employed to improve the overall performance alternating current OPF analysis. An invasive weed optimizer (IWO) was presented in [28] to combinational approach for OPF research with the inclusion of FACTs while an Emended Crow Search Algorithm (ECSA) was utilized on the OPF with adjustments involving a novel bat technique [29]. A placement methodology for TCSC in power systems that takes into account both line interruptions and normal operation was developed in [30]. In order to minimize the power system's voltage stability index, voltage deviation and power loss, the stochastic OPF problem has been handled in [31] with the use of an adaptive Lightning Attachment Procedure Technique (ALAPT) with the inclusion of renewable sources. In [32], the impact of hydro constraints has been investigated in the operation of hydrothermal systems via a nonlinear multi-period hydrothermal OPF model. While the study resulted in a notable reduction in transmission line overloads during the IEEE 5 bus and 14 bus networks, it failed to determine the appropriate TCSC sizing in the investigated networks, which has a significant impact on these applications. In [33], the OPF has been solved by the error bound which could be represented by greatest discrepancy between the best possible outcomes of OPF models. In [34], Social Network Search Approach (SNSA) has been employed on a multi- OPF and applied on practical electrical system. Gorilla Troops Technique (GTT) was carried out on the IEEE 30 bus grid in [35] and addition of TCSC modules to the IEEE 30 bus system in [36]. However, the allocation and size of the TCSC devices have not been studied. To increase the voltage stability and available transfer capability, a multi-objective PSO for the multi-objective optimal allocation model for TCSC has been performed in [37]. This study presented a chaos initialization approach and then set up a variable inertia weight configuration for the IEEE-30 bus system, which can only be used to one transmission network. To find the best position and compensation level of TCSC devices, an enhanced version of GA was presented in [38]. To improve the transfer capacity that is accessible in power systems, the proposed GA was integrated with twofold mutation probabilities. A modified version of Subtraction-Average-Based Optimizer (SAO) for TCSC allocation, which lessens losses in electric power grids, is provided in [39]. This study modifies the usual SAO by incorporating a cooperative learning strategy powered by the leader solution.

To obtain OPF solutions, the authors employed an improved particle swarm optimization technique. The OPF of IEEE 30- and 57-bus networks provided with TCSC and TCPS was carried out in [40]. The analysis considered the positions of the FACTs devices to be fixed. Improved particle swarm optimisation was used in [41] to solve the OPF created with serial FACTs devices, where it was capable of handling challenging OPF situations. Using a generalized interline power flow controller (GIPFC), the OPF problem has been tackled in [42] and improved the efficiency of the current transmission lines. Employing the ameliorated ant lion optimization technique, the authors were able to find the solutions for the OPF modeled with FACTs. To generate high-quality OPF solutions, the success history-based adaptive differential evolution (SHADE) technique has been combined with the overpowering of feasible solutions constraints addressing strategy. Using the adaptive parallel seeker optimization technique, OPF solutions have been achieved in [43] while taking into account the best possible allocation of TCSC. Case studies with OPF were conducted under both nominal and contingency settings. Numerous methods exhibit remarkable convergence characteristics and proficiently establish inequality bounds. Nonetheless, these conventional strategies are susceptible to getting trapped in local minima due to their reliance on the initial setup, rendering them incapable of attaining the true optimal outcome. Furthermore, while dealing with discrete and integer variables, each technique struggles and necessitates modelling specific versions of the OPF. Therefore, creating metaheuristic methods is crucial to getting over the restrictions mentioned above [44].

In order to enhance the power system available transfer capability, optimizing the TCSC parameters and places was addressed for mitigating the network congestion [45]. The system's sensitivity to parameter changes was estimated in this study using sensitivity factor-based approaches. These approaches, nevertheless, are limited to linear approximations of system behaviour and may occasionally fail to identify the globally best solution, which could end up to inadequate outcomes in nonlinear systems. Sensitivity-based approaches are therefore less effective when many TCSCs are needed to relieve electrical grid congestion. Several heuristic/metaheuristic techniques can be used to concurrently locate and optimise TCSCs in order to overcome this problem. In [46], the integration of FACTs devices into the system has been coded using Newton Raphson load flow equations to determine their optimal locations while a heuristic optimization algorithms in [47] has been adopted to identify suitable locations for FACTs devices and optimize their parameters. In [48], a GA has been designed to optimize a nonlinear objective function, focusing on the practical incorporation of FACTs devices within a congested network. In [49], Teaching-Learning-Based Optimizer (TLBO), Gray Wolf Optimizer (GWO) and Particle Swarm Optimizer (PSO) have been applied and compared for optimizing the TCSC reactance for stable system operation and congestion mitigation. In this study, the suitable locations were determined in a separate pre-stage employing the line utilization factors. Thereafter, TLBO, GWO and PSO have been contrasted with the application on the standard IEEE-30 bus system where the findings indicated that TLBO provided better performance than PSO and GWO. Unfortunately, because the pre-specified TCSC placement using the line utilisation factor was predicated on a single static operating situation, it might not be able to adjust efficiently to changes in real time brought about by fluctuating loads and generation patterns. Under the changed circumstances in the power system, this static placement might not be beneficial. Additionally, under certain operating conditions, the pre-specified placements might not always find the best places to mitigate congestion, which could result in suboptimal performance in congestion management and voltage stability.

This study demonstrates an Enhanced Gradient-Based Algorithm (EGBA) incorporating the Gradient Search Process (GSP) and Local Escaping Process (LEP) for handling different benchmark functions and the TCSC optimal allocation issue. The exceptional indicated solution contains GSP and LEP to guide the exploration process and prevent premature convergence to suboptimal solutions. Initially, the effectiveness of the proposed EGBA and GBA is evaluated using the CEC 2017. Besides, to assess the practical applicability of the proposed EGBA is specifically implemented for the optimal allocation of TCSC devices to minimize technical power losses in transmission power systems. Furthermore, the accuracy and superiority of the proposed EGBA over the others can be observed while considering a range of TCSC devices.

- A new metaheuristic approach called EGBA is developed.
- The EGBA algorithm is utilized to determine the best placement and rating for TCSC devices that are integrated with the IEEE 30-bus and IEEE 57-bus power network.
- It is successfully implemented for enhancing power system performance via TCSC allocation under varying numbers of TCSC devices.
- Additionally, the goal of improving the security margin of transmission lines is incorporated to optimize power flow, alongside the objective of minimizing power losses.
- The voltage profile is further improved for all buses based on the proposed EGBA with average improvement of 7.22% and 8.08% for both systems.
- The results of the simulation reveal that the proposed EGBA outperforms many other modern alternatives as well as the original GBA in terms of effectiveness and efficacy. Also, the proposed method is proven to be superior by the statistics and convergence analysis results considering CEC 2017 benchmark functions.

The following is the structure of the remaining portions of the paper: The approach to use for minimizing power losses when TCSC devices are present is discussed in Section II. The optimization frameworks for the original GBA and its improved version (EGBA) are provided in Section III. The simulation findings, which are divided into two subsections, are presented in Section IV. The experimental research conducted to identify the optimal EGBA version is covered in the first subsection. The allocation and size problem for TCSC devices to lower the power network losses is provided in the second subsection. This solution is derived using the suggested EGBA and additional competitive metaheuristic algorithms. The findings of the current study are discussed in Section V.

II. PROBLEM FORMULATION: TCSC ALLOCATION IN TRANSMISSION NETWORKS

A. TCSC MODELING

Among the various FACTs devices, the TCSC stands out as a popular choice due to its numerous benefits. These benefits include its effectiveness, rapid response time, and cost-efficiency [50]. The TCSCs can operate in two modes: inductive and capacitive, allowing them to either increase or decrease the reactance of a transmission line. Figure 1(a) illustrates how a TCSC is connected in series with a transmission line within a power network. Its internal structure consists of a capacitor (C) in parallel with an inductor (L), with their combined behavior controlled by a thyristor-based valve. The valve's operation is determined by the extinction angle (α), which can be adjusted within a range of 90° to 180° [51]. The TCSC compensator acts as a variable capacitor, changing the reactance (resistance to AC current) of the transmission line as depicted in Fig. 1(b) [52]. Essentially, the TCSC's reactance replaces the original reactance of the transmission line (X_{Line}). To avoid overcompensating the line, the necessary X_{TCSC} value can be calculated using a specific equation [53].

$$X_{TCSC}(\alpha) = \frac{X_L(\alpha) \times X_C}{X_L(\alpha) + X_C} \tag{1}$$

$$X_L(\alpha) = \left(\frac{\pi}{\pi - sin(2\alpha) - 2\alpha}\right) X_{L,max} \tag{2}$$

$$X_{L,max} = (2\pi f)\, L, \;\; X_C = \frac{-1}{j\,(2\pi f)\, C} \tag{3}$$

By replacing the terms $X_L(\alpha)$ and X_C, the formulation of Eq. (1) becomes as follows:

$$X_{TCSC}(\alpha) = \frac{\left(\frac{\pi}{-2\alpha - sin(2\alpha) + \pi}\right) X_{L,max} \times X_C}{X_C + \left(\frac{\pi}{-2\alpha - sin(2\alpha) + \pi}\right) X_{L,max}} \tag{4}$$

B. LOSSES MINIMIZATION AND CONSTRAINTS

Reducing total network losses is the main objective since it improves voltage profile and electrical system performance. For computing purposes, this objective function (OF) can be mathematically described as follows [55]:

$$P_{Loss} = \sum_{m=1}^{Nbus} \left(\sum_{\substack{n=1 \\ m \neq n}}^{Nbus} G_{mn} \left(V_m^2 - 2 \times \left(V_m V_n cos\,(\theta_{mn}) + V_n^2 \right) \right) \tag{5}$$

where the variables θ_{mn} and V_{mn} indicate the phase angle and voltage difference, respectively, between buses m and n, while N_{bus} denotes the number of buses. Moreover, G_{mn} indicates the conductance of the transmission line connecting buses m and n.

Lots of equality and inequalities constraints pertaining to both dependent and independent variables must be satisfied in order to address the TCSC allocation problem.

The following are the control variables for optimum TCSC allocation challenges:

1. Reactance compensation for each TCSC device that needs to be deployed.
2. Each TCSC device that is installed will require the selection of potential transmission lines.
3. Injecting reactive power into the transmission system with the use of current Var sources.
4. The voltage of the generator
5. The output powers of the generator.
6. Transformer tap configurations.

Therefore, Equations. (6) and (7) indicate that the specifications for reactance compensation, independent variables, and TCSC places are required to be satisfied.

$$-50\% X_{Line_{TCSC,k}} \geq X_{TCSC}(\alpha)_k \geq +50\% X_{Line_{TCSC,p}}, \quad k = 1, 2, \ldots N_{TCSC} \tag{6}$$

$$N_{lines} \geq Line_{TCSC,k} \geq 1, k = 1, 2, \ldots N_{TCSC} \tag{7}$$

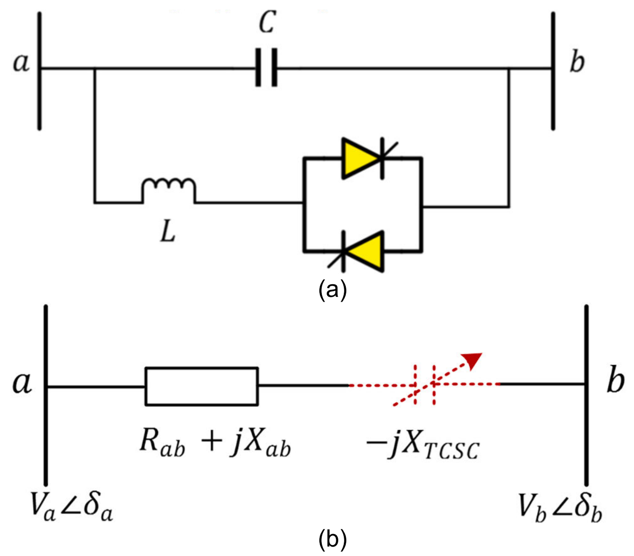

FIGURE 1. (a) TCSC Circuit model (b) Configuration of transmission line with TCSC [54].

where $Line_{TCSC,k}$ refers to the potential lines for fixing TCSC devices; N_{lines} expresses the entire number of transmission lines; N_{TCSC} signifies the entire number of allocated TCSC devices; $X_{Line_{TCSC,k}}$ designates the reactance of the corresponding lines which are designated for fixing TCSC device.

Regarding independent variables, Equations (8)–(11) control the limitations for tap settings, generator output powers, generator voltage, and reactive power injection from Var sources, respectively [56].

$$Tp_k^{min} \leq Tp_k \leq Tp_k^{max}, k = 1, 2, \ldots Nt \quad (8)$$
$$Pgn_m^{min} \leq Pgn_m \leq Pgn_m^{max}, m = 1, 2, \ldots Ngn \quad (9)$$
$$Vgn_m^{min} \leq Vgn_m \leq Vgn_m^{max}, m = 1, 2, \ldots Ngn \quad (10)$$
$$QI_{Vr}^{min} \leq QI_{Vr} \leq QI_{Vr}^{max}, Vr = 1, 2, \ldots Nq \quad (11)$$

where Nq designates the entire number of VAr sources, Ngn indicates the entire number of generation plants, and Nt stands for the entire number of transformers. Pgn describes the real generators' power output; Tp reveals the tap values that describe the tap transformers. Besides, the two symbols Vgn and QI illustrate the generators' voltages and the reactive power that are injected by VAr sources, respectively.

Furthermore, with regards to dependent variables, the restrictions pertaining to apparent power flow across the transmission lines, bus voltage, and generators' reactive power output are handled by Eqs. (12)–(14).

$$|SF_L| \leq SF_L^{max}, L = 1, 2, \ldots N_{lines} \quad (12)$$
$$V_m^{min} \leq V_m \leq V_m^{max}, m = 1, 2, \ldots Nbus \quad (13)$$
$$Qg_m^{min} \leq Qg_m \leq Qg_m^{max}, m = 1, 2, \ldots Ng \quad (14)$$

where SF signifies transmission flow constraints and Qg indicates the generators' reactive power.

While minimizing network losses, it's crucial to maintain the balance between active and reactive power at each bus in the system. This balance is ensured by fulfilling specific equality constraints, which are achieved through the execution of a load flow analysis.

III. PROPOSED EGBA FOR OPTIMAL TCSC ALLOCATION IN POWER SYSTEMS

The GBA serves as a powerful metaheuristic approach adept at addressing intricate optimization problems through the amalgamation of population-based and gradient-based methodologies [57]. Within this framework, the navigation of search agents in the problem space is orchestrated by Newton's method, a technique intricately woven into the structure of the GBA [58]. In an effort to refine and amplify this methodology, an innovative adaptation EGBA is introduced. The proposed EGBA distinguishes itself by seamlessly integrating a crossover strategy into the foundational GBA structure, thereby enriching the diversity exhibited by the generated search agents. This advanced design incorporates a crossover strategy, contributing to the creation of a more diverse and randomly configured population in subsequent iterations. Crucially, the essential elements of the GSP and LEP, inherent in the GBA, remain integral to the proposed EGBA. The deliberate retention of these core mechanisms ensures that the modified version upholds the fundamental principles of directing the search toward promising areas and circumventing entrapment in local optima.

A. INITIALIZATION

The commencement of the EGBA involves the initiation of a set of initial search solutions, each evolving with respect to its position along a path determined by gradients. The maximum number of iterations is denoted by t_{Mx}. This process is articulated through the following expression:

$$X_k = X_{Mn} + rd_0 \times \left(X_{Mx} - X_{Mn}\right); k = 1 : N_x \quad (15)$$

Here, the notation X_k represents each searching individual within the population, and "X_{Mn}" and "X_{Mx}" denote the lower and upper boundaries of the dimensions (Dim), respectively. rd_0 represents a randomly generated values within the boundary [0,1]. N_x denotes the count of search individuals within the population. This initialization stage marks the inception of the EGBA algorithm, setting the groundwork for subsequent gradient-guided movements of the search individuals within the defined solution space.

B. GSP EXPLORATION AND CONVERGENCE ENHANCEMENT

The GSP is harnessed within the optimization framework to augment the exploration of the scanning universe and expedite the convergence towards the optimal solution. This method leverages gradient-based techniques to guide the search process effectively. The iterative refinement of findings in each cycle is accomplished through the application of the following mathematical expression:

$$X_k^* = rd_1 \left((1 - rd_2)A_k + rd_2 B_k\right) + (1 - rd_1)C_k; k = 1 : N_x \quad (16)$$

In this equation:

X_k^* and X_k correspond to the updated and previous solution vectors associated with the solution position.

rd_1 and rd_2 represent two randomly generated values within the boundary [0,1].

A, B and C denote three newly assessed solutions, calculated as follows:

$$A_k = X_{Best} + rand \times \sigma_1 \times (X_{R1} + X_{R2}) - GSP; k = 1 : N_x \quad (17)$$

$$B_k = X_k + rand \times \sigma_1 \times (X_{Best} + B_k) - GSP; k = 1 : N_x \quad (18)$$

$$C_k = B_k + \sigma_2 \times (A_k - B_k); k = 1 : N_x \quad (19)$$

$$GSP = \sigma_1 \times randn \left(\frac{2 \times X_k \times \Delta X}{\varepsilon + yp_j - yq_j}\right) \quad (20)$$

Here:

σ_1 is a pivotal parameter subject to variations based on the sine function.

σ_2 represents a randomized parameter.

randn and rand denote a generated integer number and a uniformly distributed generated number within the boundary [0,1].

X_{Best} symbolizes the optimal searching solution yielding the minimum objective score.

X_{R1} and X_{R2} illustrate two randomly chosen and distinct solutions.

This intricate process, involving the exploration and convergence-enhancing mechanisms of the GSP, demonstrates the sophistication and adaptability embedded within the EGBA method for optimization endeavors.

C. LEP FOR AVOIDING LOCAL OPTIMA

The LEP is a crucial component employed within the optimization framework to steer the program away from local optima, thereby enhancing the algorithm's adaptability. Following each iteration, the EGBA method refines its findings through the utilization of the ensuing mathematical formulation:

$$X_k^* = \left\{ \begin{array}{ll} X_k^* + D_k + L_2 (X_{R1} - X_{R2}) & if\ rd_3 < 0.5 \\ X_k^* + D_k + \frac{L_2}{2} (X_{R1} - X_{R2}) & Else \end{array} \right\} \ if\ rd_4 < \Psi \tag{21}$$

$$D_k = \phi_1 (L_1 X_{Best} - L_2 X_k) + \sigma_1 \phi_2 (L_3 A_k - B_k) \tag{22}$$

In this expression:

Ψ signifies the likelihood of activating the LEM step.

rd_3 and rd_4 are random values within the range [0,1].

ϕ_1 and ϕ_2 represent two randomly generated values using a uniform distribution function within the interval $[-1, 1]$.

L_1, L_2, and L_3 are three random numbers produced through the following equations:

$$L_1 = (2 \times \zeta \times rd_5) - (\zeta - 1) \tag{23}$$

$$L_2 = (rd_5 \times \zeta) - (\zeta - 1) \tag{24}$$

$$L_3 = (rd_5 \times \zeta) - (\zeta - 1) \tag{25}$$

$$\zeta = \begin{cases} 0 & M_1 > 0.5 \\ 1 & Else \end{cases} \tag{26}$$

Here, M_1 indicates a randomly generated number within the set [0,1].

$$X_k = \begin{cases} X_{R3} & if\ M_2 < 0.5 \\ X_{Mn} + rd_0 \times \left(X_{Mx} - X_{Mn}\right) & Else \end{cases} \tag{27}$$

D. CROSSOVER STRATEGY INCORPORATION

In this research endeavor, an advanced EGBA is introduced, featuring an augmented crossover operator seamlessly integrated with the original EGBA. This augmentation is designed to significantly enhance the diversity of the solutions generated by the algorithm. The application of the crossover operator is strategically orchestrated for each solution in every iteration, contingent upon a predefined crossover probability. The operational paradigm of the crossover operation unfolds as follows:

TABLE 1. Parameters of the compared algorithms.

Algorithm	Parameters
GBA	N_x=30; t_{Mx}=500; Ψ=0.5.
Proposed EGBA	N_x=30; t_{Mx}=500; Ψ=0.5; Cr_p =0.25.
DMO (2022) [66]	Maximum number of iterations = 500; Number of dwarfs = 30; Number of babysitters = 3; Alpha vocalization (peep=2)
AOT (2021) [61]	Number of iterations = 500; Number of Aquila = 30; Alpha parameter = 0.1; Delta parameter = 0.1
GTT (2021) [67]	Number of iterations = 500; Number of gorillas= 30.
RKA (2022) [63]	Number of iterations = 500; Number of searching agents= 30
SAO (2023) [64]	Number of iterations = 500; Number of searching agents= 30

$$X\_new_{k,j} = \begin{cases} X_{SR,j} & if\ rd_6 < CR_p \\ X_{k,j}^* & Else \end{cases}$$
$$k = 1 : N_x; j = 1 : Dim \tag{28}$$

where , X_new corresponds to the new generated solution position; X_k^* stands for the upgraded one after either the GSP as activated in Eq. (15) or the LEP as activated in Eq. (21) while X_k is the previous solution position. CR_p indicates the crossover probability while rd_6 is a randomly generated values within the boundary [0,1].

Based on that model, a new solution vector is synthesized by exchanging components between the current upgraded solution vector and a randomly selected one from the population. The activation of this crossover operation is governed by a condition based on the crossover probability (CR_p) which is set in this study to 25%. Consequently, a random value (rd_6) within the range [0,1] is generated where the crossover is employed when it is less than crossover probability, showcasing a judicious selection criterion. On the other side, any dimension of the new generated solution position (X_new) may exceed the permissible limit. Therefore, each dimension should be preserved if it is exceeded. The mathematical representation of the preservation mechanism is encapsulated in the following expression:

$$X\_new_{k,j} = \begin{cases} X_{Mn,j} & if\ X\_new_{k,j} < X_{Mn,j} \\ X_{Mx,j} & if\ X\_new_{k,j} > X_{Mx,j} \\ X\_new_{k,j} & Else \end{cases}$$
$$k = 1 : N_x; j = 1 : Dim \tag{29}$$

E. OBJECTIVE EVALUATION AND CONSTRAINTS HANDLING OF TCSC ALLOCATION IN POWER SYSTEMS

In addressing the TCSC allocation problem, due consideration is accorded to both equality and inequality constraints. To satisfy the equality criteria inherent in load flow balancing equations, the Newton-Raphson (NR) technique is employed. This technique is particularly significant in power network engineering as it upholds power balancing requisites, portraying the system's steady state. Consequently, the NR approach

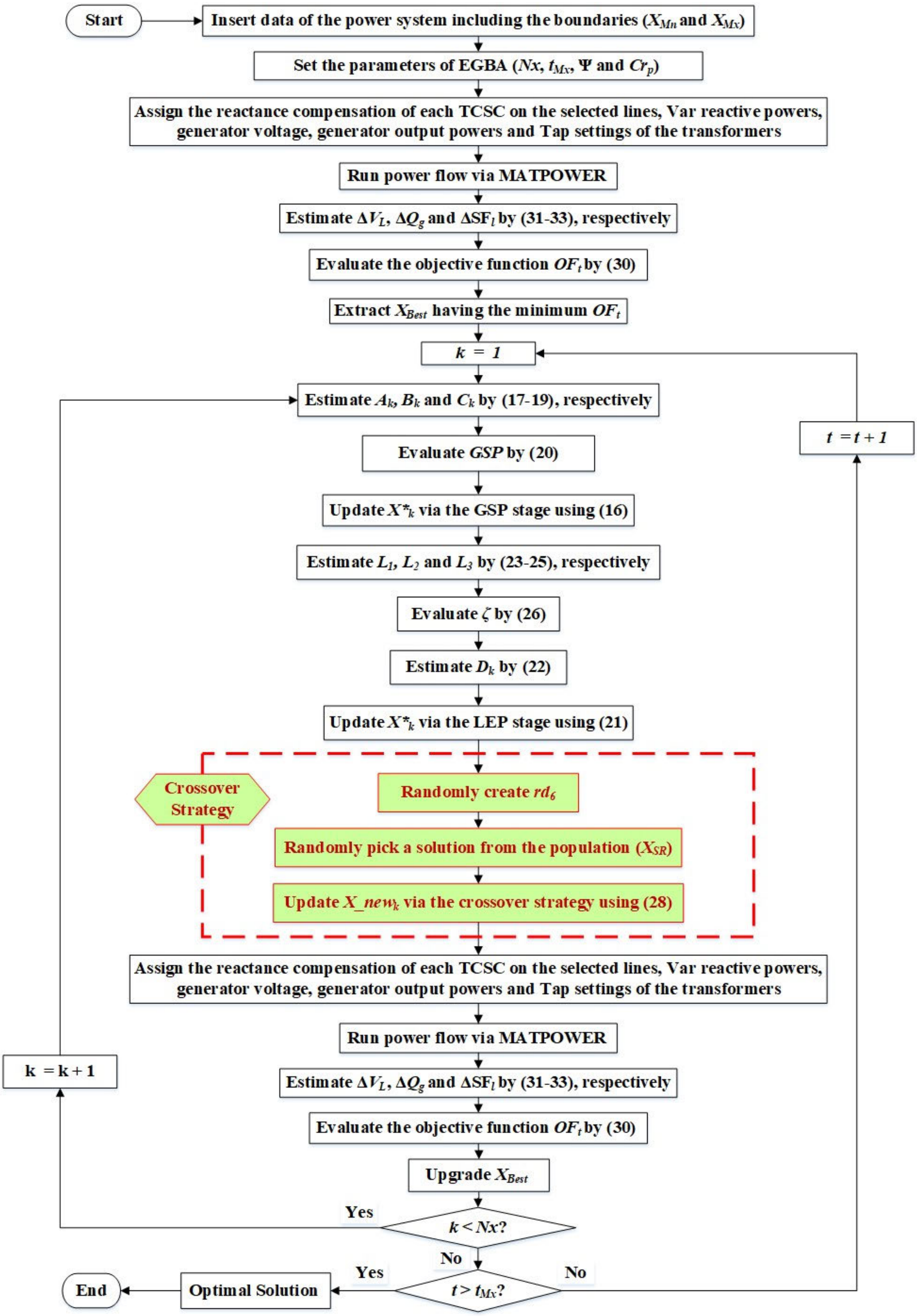

FIGURE 2. EGBO flowchart.

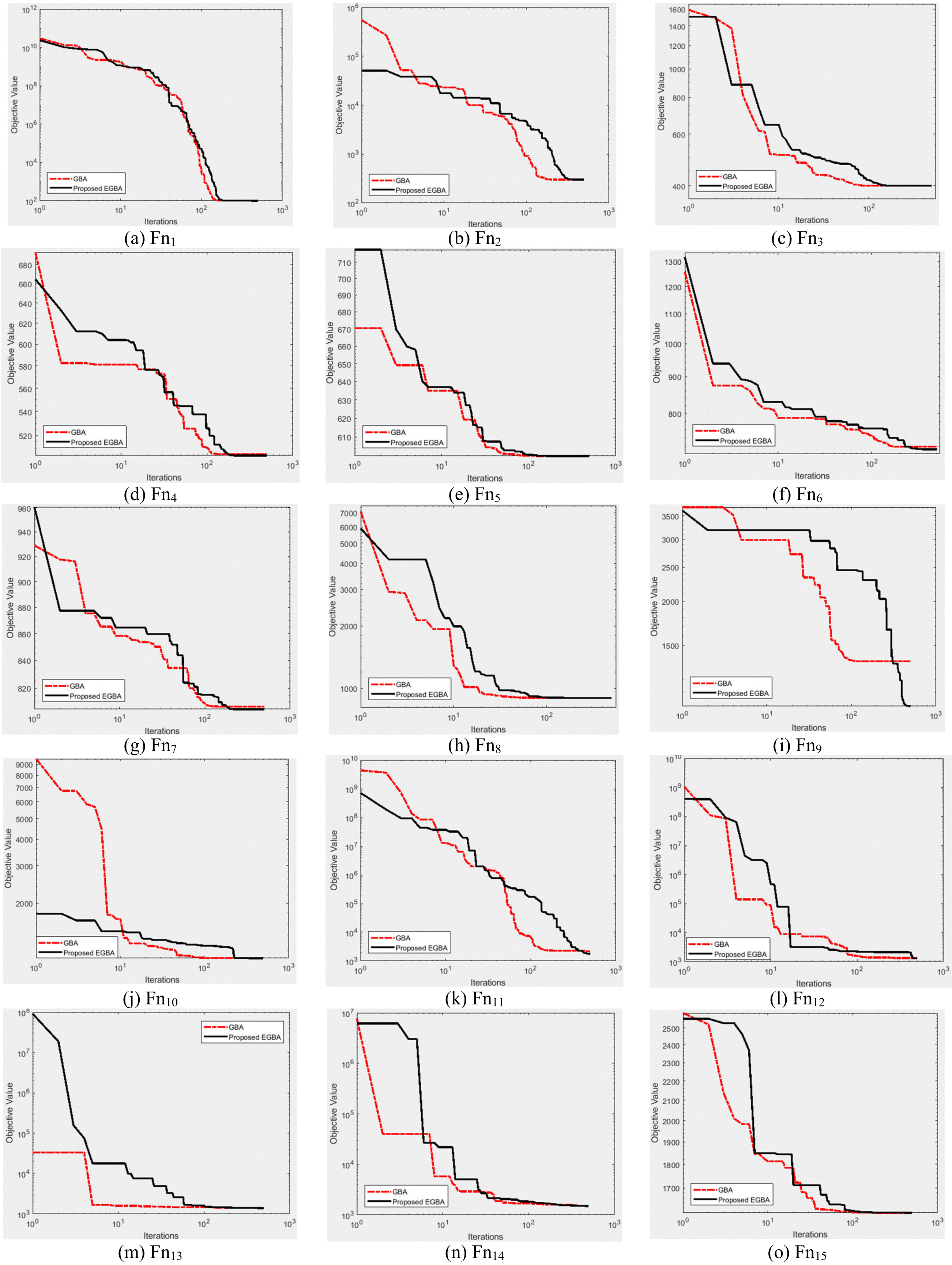

FIGURE 3. Converging trends of EGBA and GBA for CEC 2017 benchmarks.

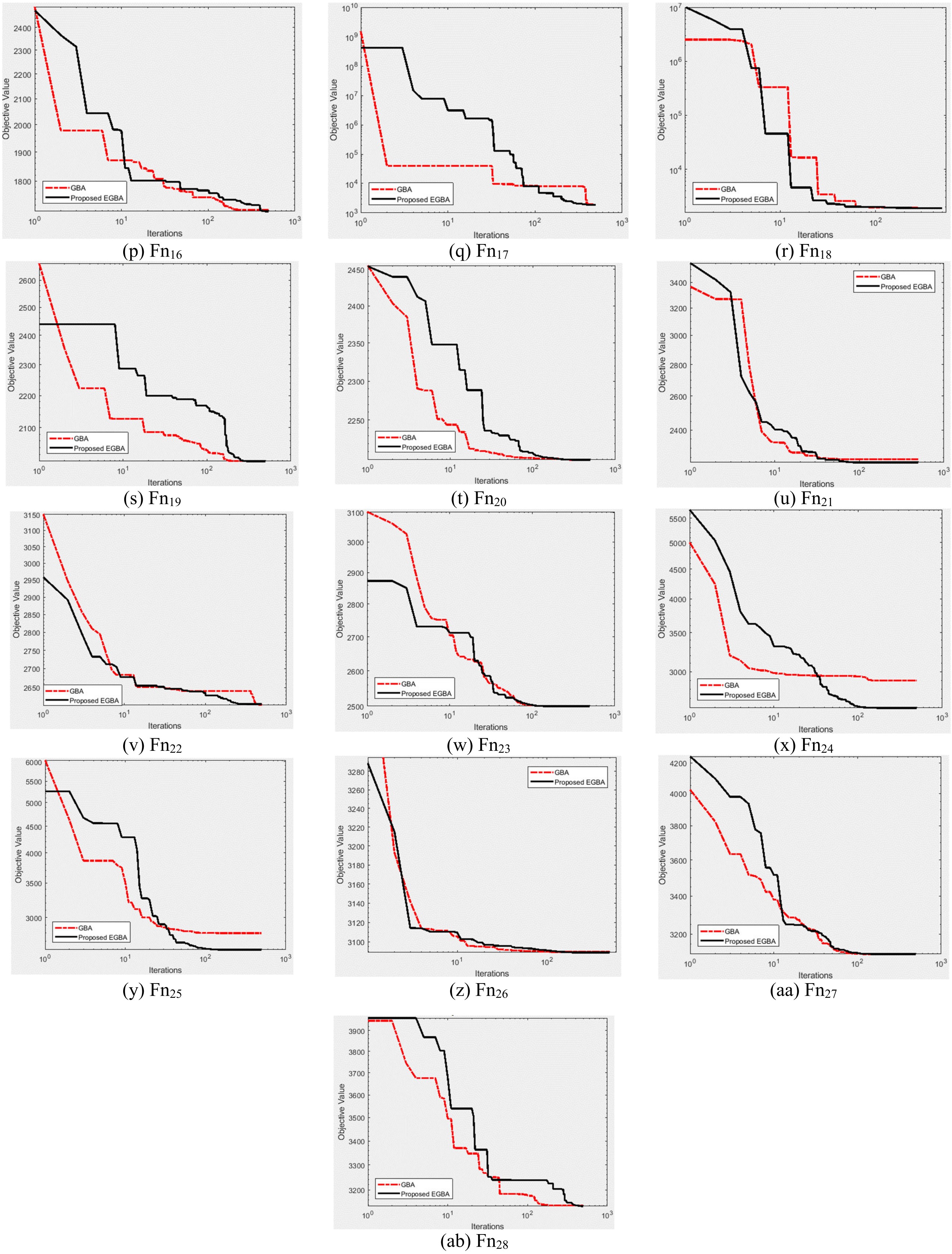

(p) Fn_{16} (q) Fn_{17} (r) Fn_{18} (s) Fn_{19} (t) Fn_{20} (u) Fn_{21} (v) Fn_{22} (w) Fn_{23} (x) Fn_{24} (y) Fn_{25} (z) Fn_{26} (aa) Fn_{27} (ab) Fn_{28}

FIGURE 3. ***(Continued.)*** **Converging trends of EGBA and GBA for CEC 2017 benchmarks.**

TABLE 2. Statistical indices of EGBA, GBA, GTT, DMO, SAO, RKA and AOT for CEC 2017 problems.

No.	Function	Index	Proposed EGBA	GBA	GTT	DMO	SAO	RKA	AOT
Fn_1	Shifted and Rotated Bent Cigar	Best	100.029	103.4295	102.2414	103.1033	106.8504	101.3583	631630.4
		Mean	264.382	3766.844	3185.564	4947.712	3812.14	6394.494	7117627
		Worst	3839.342	11848.74	12581.75	63834.88	12866.27	12725.47	47965063
		Std	535.6324	3483.475	3349.887	12150.27	3324.979	4340.656	8879770
Fn_2	Shifted and Rotated Zakharov	Best	300.0001	300	300	426.9525	433.8029	301.5553	862.8424
		Mean	300.2544	300.0001	300	1075.823	1892.281	1791.484	14241.48
		Worst	303.7947	300.0014	300.0013	2487.439	20047	28092.82	78883.29
		Std	0.67591	0.000245	0.000183	420.1405	2775.047	4446.282	17008.76
Fn_3	Shifted and Rotated Rosenbrock's	Best	400.2089	400.0025	401.2798	400.5637	403.8382	405.4006	402.9141
		Mean	405.2743	402.6074	422.5109	405.2926	410.8517	450.0849	418.5362
		Worst	465.3209	408.1492	481.1919	406.8646	496.1308	905.8536	576.6982
		Std	8.815605	1.690257	24.41179	1.199943	18.50037	78.84186	29.72566
Fn_4	Shifted and Rotated Rastrigin's	Best	503.9798	504.9748	503.9798	518.0095	511.9395	502.097	514.84
		Mean	515.9265	524.4317	525.483	530.0403	535.7457	516.5253	528.8363
		Worst	533.8285	550.7423	552.7323	539.6044	577.6057	543.6022	552.2148
		Std	6.480707	11.09041	10.33986	5.370918	16.49356	10.16285	9.884062
Fn_5	Shifted and Rotated Expanded Scaffer's F6	Best	600	600.0018	600.4136	600	603.8165	600	607.8623
		Mean	600.006	600.6981	607.1628	600	617.543	600.623	616.8517
		Worst	600.1245	609.7719	628.7749	600.0001	647.1749	617.8881	636.7507
		Std	0.018478	1.912042	6.537381	1.77E-05	9.427292	2.806871	6.212097
Fn_6	Shifted and Rotated Lunacek Bi_Rastrigin	Best	713.2065	719.3552	720.3034	728.6148	721.5113	714.6422	728.4909
		Mean	725.0289	736.4394	751.6431	743.0721	751.7038	734.864	760.7281
		Worst	740.3079	760.9609	787.9011	753.9905	791.7054	761.6374	812.3142
		Std	6.954123	10.19635	15.84439	5.371381	18.37205	12.40402	18.5329
Fn_7	Shifted and Rotated Non-Continuous Rastrigin's	Best	804.9748	806.9647	810.9445	811.2899	805.9697	803.0511	812.173
		Mean	816.0689	823.9589	824.9637	829.6501	822.3442	813.5723	828.0318
		Worst	835.1957	849.7478	847.7579	841.7104	841.7882	837.339	846.8473
		Std	6.796644	10.25201	8.023857	6.106073	7.530569	9.903987	7.133653
Fn_8	Shifted and Rotated Levy	Best	900	900	902.6364	900	910.5194	900	935.9179
		Mean	900.3347	909.6323	951.3241	900	1080.856	900.9298	1080.06
		Worst	903.1558	967.1283	1195.189	900	1895.92	918.829	1358.738
		Std	0.621512	15.90919	64.66907	2.53E-09	170.4958	2.873668	93.07999
Fn_9	Shifted Rotated Schwefel's	Best	1006.98	1350.822	1224.032	1615.589	1221.682	1382.47	1282.538
		Mean	1533.918	1807.863	2005.585	2276.483	2024.885	1809.26	1898.988
		Worst	2159.758	2871.377	2757.256	3533.997	3318.621	2535.195	2405.251
		Std	262.0174	312.491	309.5439	277.9387	370.4943	324.4173	239.4575
Fn_{10}	Hybrid 1 (N = 3)	Best	1101.036	1102.985	1103.123	1103.032	1103.253	1101.18	1126.013
		Mean	1107.793	1120.713	1136.846	1107.101	1158.702	1152.762	1245.853
		Worst	1118.704	1173.627	1474.95	1112.527	1273.258	1361.733	1543.506
		Std	4.968793	15.25929	52.57824	2.507902	43.42037	85.62553	95.9905
Fn_{11}	Hybrid 2 (N = 3)	Best	1735.766	2104.752	2251.604	7581.318	2220.099	11046.39	59003.65
		Mean	18642.6	17326.59	19484.78	147990.2	16173.04	556267.5	5839942
		Worst	61079.09	59653.42	52538.98	848651.8	53781.33	15705336	21294607
		Std	17623.1	14977.25	14651.39	157984.9	13805.32	2309722	6235390
Fn_{12}	Hybrid 3 (N = 3)	Best	1309.588	1318.271	1301.353	1471.087	1521.598	1596.162	2983.547
		Mean	1396.174	2157.343	1661.761	4806.373	11073.28	12489.74	16104.91
		Worst	1669.792	4914.884	2445.92	14058.03	36272.32	72354.44	57140.58
		Std	74.98543	778.7237	301.6881	2962.256	9503.086	11704.68	11977.37
Fn_{13}	Hybrid 4 (N = 4)	Best	1401.066	1426.051	1413.99	1437.532	1451.43	1468.283	1475.86
		Mean	1424.039	1492.015	1461.535	93986408	3218.386	1594.974	2726.689
		Worst	1449.941	1592.383	1513.531	3.81E+09	14794.43	2492.51	7300.955
		Std	11.67887	42.13764	27.67236	5.51E+08	2633.219	161.0686	1181.206
Fn_{14}	Hybrid 5 (N = 4)	Best	1502.157	1515.753	1503.209	1574.339	1562.425	1666.848	1704.87
		Mean	1516.412	1671.866	1586.639	1894.31	3284.562	2545.096	7155.795
		Worst	1565.793	1958.191	1860.807	2742.553	5926.97	4767.804	13013.25
		Std	12.69383	101.503	74.26103	289.9846	1216.997	803.5599	2819.584
Fn_{15}	Hybrid 6 (N = 4)	Best	1600.868	1600.722	1601.468	1601.544	1601.703	1600.854	1625.733
		Mean	1669.566	1722.844	1700.231	1613.991	1817.625	1632.426	1799.318
		Worst	1950.653	1989.521	1992.801	1738.793	2135.552	1900.84	2117.308
		Std	85.52583	115.3881	95.75652	22.69649	142.0484	58.07911	128.3401
Fn_{16}	Hybrid 6 (N = 5)	Best	1700.847	1705.307	1716.933	1712.647	1723.965	1706.86	1745.723
		Mean	1734.976	1745.773	1742.867	1740.727	1783.957	1742.974	1781.167
		Worst	1843.906	1864.593	1800.339	1761.893	1925.583	1781.586	1858.912
		Std	22.24198	32.8477	16.51172	9.774917	53.54611	11.82739	26.89721
Fn_{17}	Hybrid 6 (N = 5)	Best	1857.204	1911.689	1849.487	1983.072	1990.645	3489.732	6124.661
		Mean	4530.264	9294.496	4734.006	7055.869	10866.06	33008.39	45811.23
		Worst	22472.15	34757.98	34251.62	19019.33	55426.05	209371	72733.15
		Std	4551.122	10028.21	6545.115	4063.737	11000.98	34519.64	15609.74
Fn_{18}	Hybrid 6 (N = 5)	Best	1903.016	1914.292	1904.802	1911.531	2025.102	1947.243	2007.858
		Mean	1910.994	2033.453	1963.373	2172.458	11852.15	3129.286	25488.55
		Worst	1938.962	3798.903	2095.158	3884.533	208941.3	9117.7	120047.6
		Std	6.4365	269.77	53.05017	328.5189	28897.4	1670.582	21289.85

TABLE 2. Statistical indices of EGBA, GBA, GTT, DMO, SAO, RKA and AOT for CEC 2017 problems.

Fn_{19}	Hybrid 6 (N = 6)	Best	2000	2001.03	2021.732	2000.323	2031.366	2001.065	2049.27
		Mean	2015.806	2080.111	2092.222	2010.275	2146.249	2040.972	2134.692
		Worst	2048.536	2268.3	2206.172	2035.596	2324.983	2161.175	2262.899
		Std	12.86997	68.73914	53.84462	10.40192	74.54465	48.08278	56.72375
Fn_{20}	Composition 1 (N = 3)	Best	2200	2200	2200	2207.963	2200	2202.68	2206.064
		Mean	2284.208	2290.525	2217.228	2421.83	2311.109	2269.041	2303.841
		Worst	2334.152	2350.148	2342.25	3423.376	2379.046	2341.668	2348.035
		Std	52.53176	59.44758	43.09881	276.8203	53.57661	59.03082	49.8612
Fn_{21}	Composition 2 (N = 3)	Best	2223.027	2240.179	2237.236	2290.772	2244.561	2225.953	2245.189
		Mean	2300.381	2299.224	2303.812	2302.682	2309.082	2395.433	2310.746
		Worst	2305.477	2308.452	2319.036	2306.795	2345.843	3882.778	2331.133
		Std	11.21429	14.3533	10.3266	2.544353	12.51222	333.9873	14.20948
Fn_{22}	Composition 3 (N = 4)	Best	2606.265	2603.248	2607.767	2611.39	2614.191	2605.674	2614.735
		Mean	2617.473	2626.889	2623.589	2626.133	2655.502	2628.164	2639.714
		Worst	2637.999	2656.782	2683.03	2643.387	2714.223	2712.256	2680.313
		Std	7.28785	11.771	13.03785	7.061391	25.23442	25.15645	13.18305
Fn_{23}	Composition 4 (N = 4)	Best	2500	2500	2500	2529.358	2500	2737.125	2743.333
		Mean	2733.024	2749.944	2722.229	2779.46	2776.754	2760.733	2765.077
		Worst	2781.657	2785.586	2785.801	4667.793	2881.822	2862.941	2791.924
		Std	70.14732	37.45386	91.37158	403.3049	48.65351	25.74767	11.60206
Fn_{24}	Composition 5 (N = 5)	Best	2600.064	2897.743	2897.757	2898.008	2897.941	2897.94	2898.884
		Mean	2922.165	2927.384	2928.394	2923.861	2927.008	2928.859	2938.885
		Worst	2950.394	2952.709	2971.013	2945.222	2978.515	2953.657	3030.515
		Std	51.66106	23.37686	25.28154	20.46398	25.58298	24.11888	27.90755
Fn_{25}	Composition 6 (N = 5)	Best	2600	2800	2800	2606.09	2600	2900	2825.635
		Mean	2971.872	3082.698	2984.508	2865.906	3132.256	3165.254	3020.676
		Worst	3921.267	4233.601	3207.704	2900.003	4234.516	4028.093	3489.538
		Std	169.3923	338.5105	99.90624	56.84354	363.1331	384.0885	153.5662
Fn_{26}	Composition 7 (N = 6)	Best	3089.006	3089.518	3090.752	3091.548	3093.179	3089.308	3095.366
		Mean	3096.86	3110.646	3101.365	3095.589	3129.619	3099.07	3100.941
		Worst	3150.409	3198.403	3198.189	3100.03	3209.53	3197.703	3116.125
		Std	12.54906	30.34879	19.81815	1.944856	36.35269	18.70578	4.757791
Fn_{27}	Composition 8 (N = 6)	Best	3100	3100	3100	3100	2800.009	3108.935	3182.341
		Mean	3311.714	3332.005	3289.245	3191.247	3277.773	3352.853	3379.829
		Worst	3731.813	3731.813	3783.223	3411.823	3412.053	3731.813	3499.317
		Std	162.254	134.515	187.6894	88.55182	147.9899	193.3343	83.32384
Fn_{28}	Composition 9 (N = 3)	Best	3135.515	3138.664	3147.311	3186.272	3161.176	3138.465	3153.017
		Mean	3188.721	3233.098	3219.908	3223.056	3271.415	3175.727	3234.006
		Worst	3331.355	3375.497	3397.49	3265.67	3424.743	3234.517	3332.945
		Std	44.2335	59.28478	58.00608	16.49242	65.41059	24.26783	43.72574

serves as a crucial tool for illustrating three-phase circuits, prominently utilized by the MATPOWER [59] framework.

Within the scope of operational constraints, two distinct categories emerge, namely decision variables and dependent variable constraints. Decision variables persist in adhering to their defined limits, with any overruns triggering a random regeneration within the specified bounds, thereby ensuring compliance with the constraints articulated in Eqs. (6)-(11). This preservation mechanism, delineated in Eq. (29), plays a pivotal role in maintaining the integrity of the decision variables.

Moreover, the objective function, encompassing the second category of constraints related to dependent variables, is designed to extend and penalize violations. Consequently, if a solution violates any of the corresponding constraints, it faces rejection in the subsequent iteration. The objective function (OF_t), along with the overall network losses (OJ) defined in Eq. (5), can be expressed as follows:

$$OF_t = OJ + \lambda_1 \sum_{L=1}^{NLd} \Delta V_L^2 + \lambda_2 \sum_{g=1}^{Ng} \Delta Q_g^2 + \lambda_3 \sum_{l=1}^{Nlines} \Delta SF_l^2 \tag{30}$$

where, ΔV_L, ΔQ_g, and ΔSF_l are characterized by:

$$\Delta V_L = \begin{cases} V_L^{min} - V_L & if\ V_L < V_L^{min} \\ V_L^{max} - V_L & if\ V_L > V_L^{max} \end{cases} \tag{31}$$

$$\Delta Q_g = \begin{cases} Q_g^{min} - Q_g & if\ Q_g < Q_g^{min} \\ Q_g^{max} - Q_g & if\ Q_g > Q_g^{max} \end{cases} \tag{32}$$

$$\Delta SF_l = SF_l^{max} - SF_l \quad if\ SF_l > SF_l^{max} \tag{33}$$

Additionally, penalty factors, denoted as λ_1, λ_2, and λ_3, are introduced to penalize violations in load voltages, reactive outputs from generators, and line power flows, respectively. The depicted graphical representation in Figure 2 illustrates the principal stages comprising the proposed EGBA, shedding light on the key components and sequential progression integral to the methodology.

IV. SIMULATION RESULTS

In the following paragraphs, we investigate the use of the novel EGBA in two different cases. Simulations based on test functions are firstly engaged, focusing on the CEC 2017 evaluations in particular. Such simulated efforts involve a thorough contrast, comparing the EGBA's performance

TABLE 3. Outcomes of the proposed EGBA with respect to the original GBA and recent approaches for TCSC device allocations with respect to scenario 1.

	Initial scenario	AEO	SAO	GWO	AOT	DMO	GBA	EGBA
VG 1	1.05000	1.099351	1.1000	1.099568	1.1000	1.077325	1.10000	1.10000
VG 2	1.04000	1.094747	1.09755	1.095818	1.1000	1.07729	1.09757	1.09796
VG 5	1.01000	1.074308	1.079716	1.08001	1.09728	1.05654	1.07973	1.08070
VG 8	1.01000	1.083873	1.08684	1.085785	1.09288	1.066889	1.08691	1.08789
VG 11	1.05000	1.099959	1.1000	1.078706	1.1000	1.097459	1.10000	1.10000
VG 13	1.05000	1.099709	1.1000	1.081997	1.1000	1.089488	1.10000	1.10000
Ta 6-9	1.07800	1.028284	1.067173	1.025412	1.1000	0.979025	1.06560	1.05072
Ta 6-10	1.06900	0.925326	0.9000	0.961107	0.910477	0.94149	0.90001	0.91553
Ta 4-12	1.03200	0.999935	0.986297	1.008998	1.009181	0.973187	0.98716	0.98718
Ta 28-27	1.06800	0.98665	0.973996	1.00225	1.034419	0.968219	0.98077	0.98281
Qr 10	0.00000	4.152465	5.000	2.13309	5.000	2.041835	5.00000	4.99881
Qr 12	0.00000	4.930084	5.000	3.124115	3.962959	3.90699	5.00000	4.99992
Qr 15	0.00000	4.952519	4.999997	0.258411	5.000	4.341322	4.92677	4.44688
Qr 17	0.00000	4.912524	4.999982	3.793636	5.000	4.602435	4.99993	4.99998
Qr 20	0.00000	1.71465	4.081398	2.796705	5.000	3.530735	4.00144	4.12738
Qr 21	0.00000	4.899575	4.968112	4.209032	5.000	4.89273	4.99987	4.99998
Qr 23	0.00000	0.885251	2.58453	3.763496	4.881004	3.418359	2.56542	2.86040
Qr 24	0.00000	3.534451	5.000	3.481095	5.000	4.364901	4.99994	4.99986
Qr 29	0.00000	2.708482	2.275642	2.864193	3.107001	1.892259	2.28297	2.48210
PG 1	99.24000	51.4936	51.21077	62.3303	51.3952	52.61437	79.99951	79.99997
PG 2	80.00000	79.78346	80.000	79.61742	80.000	79.5501	49.99998	49.99998
PG 5	50.00000	49.86303	50.000	49.8189	50.000	49.83164	35.00000	34.99988
PG 8	20.00000	34.99899	35.000	33.99505	35.000	34.71168	30.00000	29.99993
PG 11	20.00000	29.55887	30.000	29.7921	30.000	29.72535	40.00000	39.99997
PG 13	20.00000	39.98309	40.000	37.77225	40.000	39.98591	30.00000	30.00000
TCSC location	-	28-27	28-27	4-6	6-28	10-17	28-27	28-27
TCSC Compensation	-	-49.490%	-49.998%	-35.028%	- 42.017%	-11.44%	-49.99978%	-49.98048%
Losses (MW)	5.832400	2.844	2.8217	3.035	2.990	3.019	2.8157874	2.8067281

versus several recently developed metaheuristic methods. Afterward, we extend the simulations to tackle the complexities of TCSC allocating problems in the context of power systems. the applications are implemented with focus on two IEEE standard electrical networks, with 30 and 57 buses, respectively, and assess the effectiveness of the EGBA in terms of optimizing the distribution of TCSC devices.

A. EXAMINATION OF APPLICATION PERFORMANCE UTILIZING CEC 2017 BENCHMARKS

The assessment of the effectiveness of optimization strategies necessitates a rigorous validation of their performance, and benchmark functions serve as integral tools for this purpose. This section delves into the comprehensive evaluation of the proposed EGBA and GBA by leveraging the CEC 2017 competition as a standardized benchmark [60]. This competition features an array of routines specifically crafted to appraise various attributes, encompassing diverse functions with unique characteristics. Across a spectrum of 28 benchmarking functions, our evaluation employs a dimensionality of 30 control variables, each bounded within the range of [−100, 100]. The scrutiny of the proposed EGBA extends to a comparative analysis with the conventional GBA, specifically considering the CEC 2017 benchmarks. The visual representation of the convergence characteristics of both EGBA and GBA is elucidated in figure 3. To establish a comprehensive benchmark, we extend our

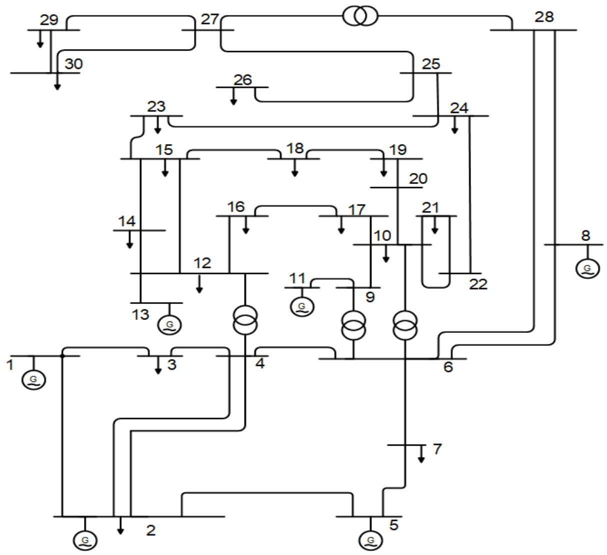

FIGURE 4. Schematic representation of the IEEE 30-bus system [70].

analysis to include a variety of contemporary optimization techniques as manifested in table 1. These encompass the Aquilla Optimization Technique (AOT) [61], GTT [62], Red Kite Algorithm (RKA) [63], and SAO [64], Slime Mould Optimizer (SMO) [65] and Dwarf mongoose optimization (DMO) [66]. The specific configurations for each method

TABLE 4. Statistical analysis of the proposed EGBA with regard to the original GBA and recent approaches for scenario 1.

	AEO	SAO	GWO	AOT	DMO	GBA	EGBA
Best	2.867	2.8217	3.035	2.990	3.019	2.8157874	2.8067281
Mean	3.007	2.930	3.472	3.080	3.065	2.8331314	2.8092166
Worst	3.180	3.188	3.849	3.172	3.109	2.8452071	2.8158849
STD	0.100	0.117	0.200	0.057	0.026	0.010732	0.0031579

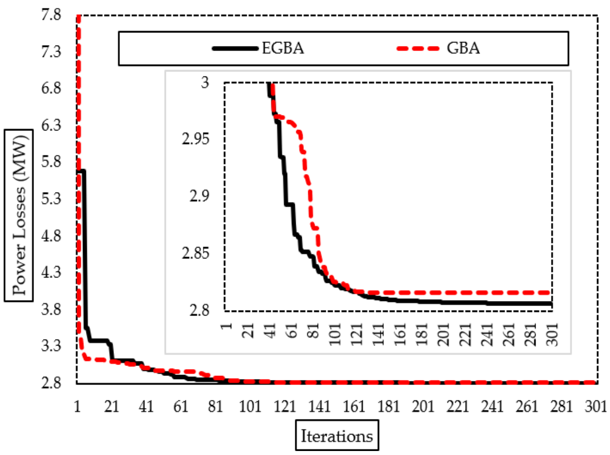

FIGURE 5. Convergence curves for the proposed EGBA versus the original GBA with respect to scenario 1.

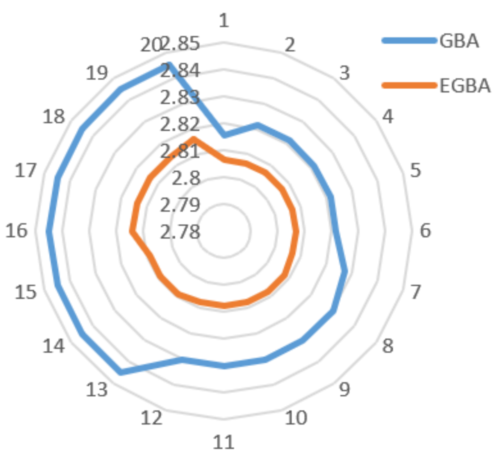

FIGURE 6. Twenty runs for outcomes of proposed EGBA with regard to the original GBA for scenario 1.

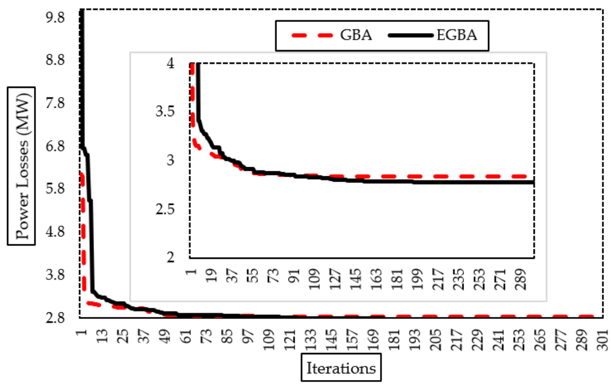

FIGURE 7. Convergence curves for the proposed EGBA versus the original GBA with respect to scenario 2.

under comparison are meticulously outlined in Table 3. In order to ensure a robust and comprehensive evaluation, a total of fifty independent operations are executed for each technique across diverse benchmarks, thereby mitigating the impact of inherent randomness. The tabulated data in Table 3 provides a comprehensive array of statistical metrics, encompassing the best, mean, worst, and standard deviation (Std) outcomes for the various techniques being compared. Notably, upon careful examination of Table 3, it becomes evident that the proposed EGBA technique demonstrates a notable superiority in efficacy, consistently registering the most favorable statistical indices across a significant majority of benchmark functions. This is highlighted by the fact that the proposed EGBA exhibits an impressive improvement percentage of 90.17% when compared to AOT. Similarly, in contrast to SAO, the EGBA method displays a substantial improvement percentage of 89.29%. Furthermore, it outperforms RKA with a noteworthy improvement percentage of 83.04%, while showcasing a commendable improvement percentage of 80.36% when compared to GBA and GTT. Finally, it demonstrates a substantial improvement percentage of 62.5% when compared to the original GBA. These results underscore the robustness and efficacy of the proposed EGBA technique, positioning it as a highly competitive and effective optimization approach when compared to a diverse set of contemporary methods across varied benchmark functions.

B. PROPOSED EGBA FOR FIXING TCSC DEVICES IN IEEE 30-BUS TRANSMISSION NETWORK

The IEEE standard 30-bus system illustrated in Fig. 4 [68] is employed in this section to manage the best TCSC allocations. This system has four parts which are 30 nodes, 41 lines, 9 compensators and 4 transformers [69]. In this system, the tap positions are 0.90 p.u. and the maximum generating voltage is 1.10 p.u. Besides, the generator bus has limits of 1.10 and 0.90 p.u, whilst the voltage limitations for the load buses are 1.05 and 0.95 p.u. The original GBA and several more modern algorithms, such as AEO, SAO, GWO, AOT and DMO, are compared with the proposed EGBA. Both implemented algorithms are run 20 times independently, with 300 iterations and 50 searching individuals for each algorithm. Three distinct situations are examined, taking into consideration one, two, and three TCSC devices, depending on the number of candidate devices provided.

TABLE 5. Outcomes of the EGBA versus the original GBA and recent approaches for TCSC device allocations with respect to scenario 2.

	Initial scenario	AEO	SAO	GWO	AOT	DMO	GBA	EGBA
VG 1	1.05000	1.099352	1.1	1.095119	1.1	1.088672	1.1	1.1
VG 2	1.04000	1.096829	1.097584	1.089415	1.1	1.084124	1.097569	1.09775
VG 5	1.01000	1.078726	1.079817	1.071614	1.1	1.063908	1.079837	1.080123
VG 8	1.01000	1.086607	1.087006	1.078618	1.094221	1.076237	1.086724	1.087352
VG 11	1.05000	1.099927	1.1	1.084584	1.1	1.098864	1.1	1.1
VG 13	1.05000	1.099558	1.1	1.074647	1.1	1.079165	1.1	1.1
Ta 6-9	1.07800	0.976591	1.064807	1.049704	1.044803	0.973169	1.067827	1.066375
Ta 6-10	1.06900	1.016372	0.900035	1.032416	0.929538	1.004953	0.900063	0.900352
Ta 4-12	1.03200	1.00762	0.980145	1.063337	1.011769	0.986186	0.987907	0.987163
Ta 28-27	1.06800	0.994596	0.980535	1.002449	1.023534	0.974498	0.980651	0.981112
Qr 10	0.00000	4.482774	5	3.497458	5	1.238543	4.99366	4.99958
Qr 12	0.00000	3.665279	5	0.832066	5	3.739474	4.998346	5
Qr 15	0.00000	3.945993	0	4.166941	4.987603	4.203835	4.995582	4.598938
Qr 17	0.00000	4.659533	5	3.173012	5	2.920776	4.989201	4.997705
Qr 20	0.00000	4.934657	5	0.851722	4.879124	4.001807	4.999066	4.263665
Qr 21	0.00000	2.590238	4.999997	3.394242	5	4.127666	4.994713	4.999404
Qr 23	0.00000	2.648497	4.274824	1.978594	5	3.891986	2.324298	2.655855
Qr 24	0.00000	4.935695	5	1.815333	5	4.158987	5	4.995292
Qr 29	0.00000	2.42653	2.352175	0.977867	5	1.801884	2.26221	2.356155
PG 1	99.24000	51.49365	51.18843	62.3303	51.39525	53.22761	79.99966	79.99962
PG 2	80.00000	79.80634	80	72.62864	80	79.01535	49.99982	50
PG 5	50.00000	49.99955	49.99428	49.966	50	49.82904	35	34.99988
PG 8	20.00000	34.98885	35	32.48052	35	34.8643	30	29.99997
PG 11	20.00000	29.99324	30	29.75128	30	29.8851	39.99993	39.99997
PG 13	20.00000	39.98501	40	39.47006	40	39.58471	1	25
First TCSC installed Lines	-	6-9	28.27	6-8	10-17	10-21	28.27	28.27
First TCSC Compensation	-	16.10%	-50.00%	24.83%	-13.64%	-13.52%	49.99996%	-49.99888%
Second TCSC installed Lines	-	4-12	6-28	16-17	6-28	15-23	2-5	2-5
Second TCSC Compensation	-	49.90%	-50.00%	-2.74%	-44.06%	23.10%	-26.00822%	-25.55362%
Losses (MW)	5.832400	2.867	2.820	3.227	2.995	3.006102	2.83880437	2.77991642

TABLE 6. Statistical analysis of the proposed EGBA with regard to the original GBA and recent approaches for scenario 2.

Algorithms	Best	Mean	Worst	STD
AEO	2.867	2.988	3.214	0.103
SAO	2.82	2.938	3.168	0.112
GWO	3.227	3.501	4.18	0.266
AOT	2.995	3.105	3.181	0.053
DMO	3.006	3.063	3.119	0.033
GBA	2.83880437	2.88131628	3.13026746	0.06456616
EGBA	2.77991642	2.7974228	2.82344339	0.01387551
AEO	2.867	2.988	3.214	0.103
SAO	2.82	2.938	3.168	0.112
GWO	3.227	3.501	4.18	0.266
AOT	2.995	3.105	3.181	0.053
DMO	3.006	3.063	3.119	0.033
GBA	2.83880437	2.88131628	3.13026746	0.06456616
EGBA	2.77991642	2.7974228	2.82344339	0.01387551

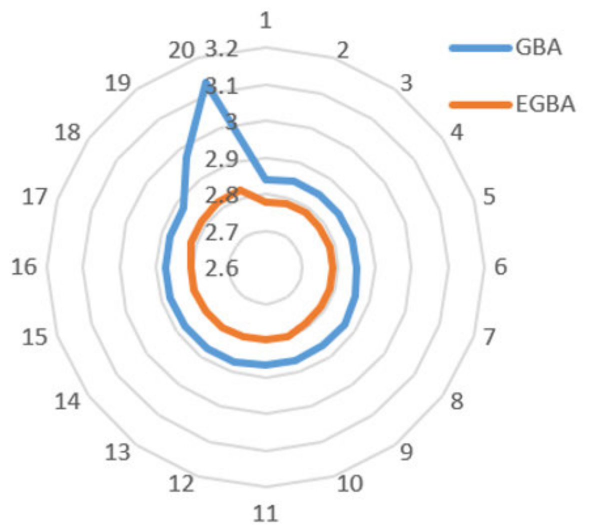

FIGURE 8. Twenty runs for outcomes of proposed EGBA with regard to the original GBA for scenario 2.

1) SCENARIO 1

The proposed EGBA is used to optimize the allocation of a single TCSC device in order to achieve lowest possible power losses. The acquired outcomes are contrasted with the original GBA, AEO, SAO, GWO, AOT and DMO. In addition to this, Table 3 displays the best control variables, which are the Var source's injection power, the output power and generators' voltage, and the tap value as well as the location and size of the TCSC device. As illustrated from this table,

TABLE 7. Outcomes of the proposed EGBA with respect to the original GBA and recent approaches for TCSC device allocations with respect to scenario 3.

	Initial scenario	AEO	SAO	GWO	AOT	DMO	GBA	EGBA
VG 1	1.05000	1.099981	1.1	1.086747	1.097922	1.086175	1.1	1.1
VG 2	1.04000	1.095393	1.1	1.082197	1.097226	1.081437	1.097873	1.097916
VG 5	1.01000	1.076605	1.082327	1.061782	1.082092	1.060443	1.079942	1.080473
VG 8	1.01000	1.083436	1.08939	1.068615	1.091701	1.065392	1.087034	1.087677
VG 11	1.05000	1.088431	1.1	1.081636	1.095909	1.096995	1.099982	1.099962
VG 13	1.05000	1.099988	1.1	1.070184	1.088444	1.090123	1.1	1.1
Ta 6-9	1.07800	0.996884	1.1	0.993708	1.01364	1.008815	1.066392	1.066091
Ta 6-10	1.06900	0.949036	0.9	1.042592	1.045173	0.946162	0.900008	0.900125
Ta 4-12	1.03200	1.031631	0.990567	1.018614	1.063428	0.975652	0.986385	0.984649
Ta 28-27	1.06800	0.976953	0.989463	0.991104	1.020301	0.983985	0.980415	0.981701
Qr 10	0.00000	4.374692	5	2.966956	5	3.411287	4.990279	4.997708
Qr 12	0.00000	4.366721	1.5E-06	0.713832	3.430701	2.250819	4.995231	4.999847
Qr 15	0.00000	4.974559	5	1.657207	1.754133	2.335161	4.971376	4.983016
Qr 17	0.00000	0.865704	5	1.784874	4.858897	3.443132	4.999992	4.995162
Qr 20	0.00000	2.802873	4.40039	2.792935	5	2.022624	4.195391	3.90454
Qr 21	0.00000	4.07292	5	1.804884	5	4.225295	4.997234	4.996962
Qr 23	0.00000	1.849487	2.71585	1.079345	5	3.516276	2.600591	2.184079
Qr 24	0.00000	4.716259	5	3.888447	5	4.033772	4.999387	4.999361
Qr 29	0.00000	2.050629	2.271475	2.454247	5	4.504769	2.220405	2.373481
PG 1	99.24000	51.43609	51.18571	56.25298	51.36892	52.70405	79.99992	79.99299
PG 2	80.00000	79.97287	80	78.58037	80	79.32674	49.99999	49.99987
PG 5	50.00000	49.99684	50	49.96991	50	49.90259	35	34.99994
PG 8	20.00000	34.99919	35	33.73529	35	34.92388	30	29.99959
PG 11	20.00000	29.97878	30	28.5719	30	29.87712	39.99997	39.99888
PG 13	20.00000	39.89602	40	39.47651	40	39.68273	30	30
First TCSC installed Lines	-	28-27	6-28	9-11	10-17	15-23	4-12	4-12
First TCSC Compensation	-	-44.65%	-36.96%	-0.62%	-39.76%	-14.12%	-50.00000	49.84641
Second TCSC installed Lines	-	6-7	10-20	12-13	6-28	16-17	28-27	28-27
Second TCSC Compensation	-	-5.97%	-50.00%	-7.28%	6.83%	-14.06%	49.99999	-49.94246
Third TCSC installed Lines	-	10-20	28-27	-	25-26	23-24	2-5	2-5
Third TCSC Compensation	-	-49.50%	-50.00%	-	-50.00%	-37.21%	50.00000	-25.20629
Losses (MW)	5.832400	2.880	2.821	3.187	2.969	3.017108	2.7996589	2.7596493

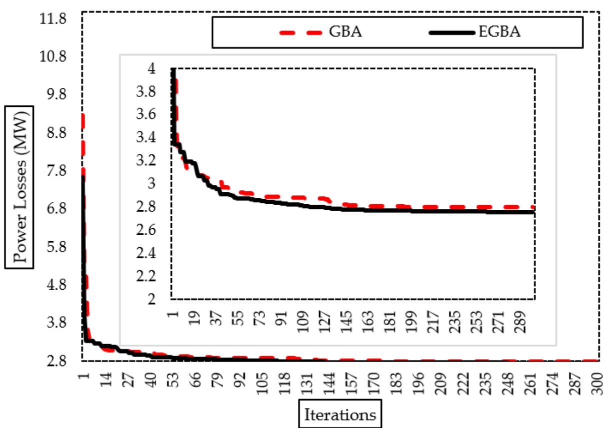

FIGURE 9. Convergence curves for the proposed EGBA versus the original GBA with respect to scenario 3.

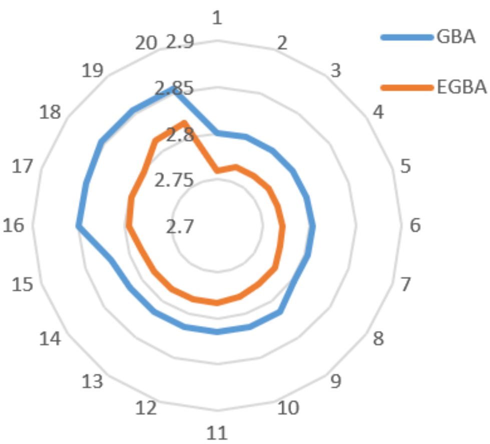

FIGURE 10. Twenty runs for outcomes of proposed EGBA with regard to the original GBA for scenario 3.

the proposed EGBA generates the least amount of power loss of 2.8067 MW. Additionally, with a −49.98 % size reduction from the installed line reactance, the transmission line (28–27) is determined to be the optimal placement for the TCSC in the proposed EGBA.

When comparing the proposed EGBA to the initial scenario, power losses were reduced by 51.88%. Moreover, the proposed EGBA achieves a noteworthy decrease percentage of 0.32% in the power losses when comparing its results with those of the original GBA. In addition, the proposed EGBA achieves a decrease percentage of over 1.33% and 0.53% in comparison to the findings achieved by the AEO and SAO. In comparison to the GWO, AOT and DMO, the proposed EGBA reduces power losses by 8.13%, 6.53%. and 7.56%, respectively.

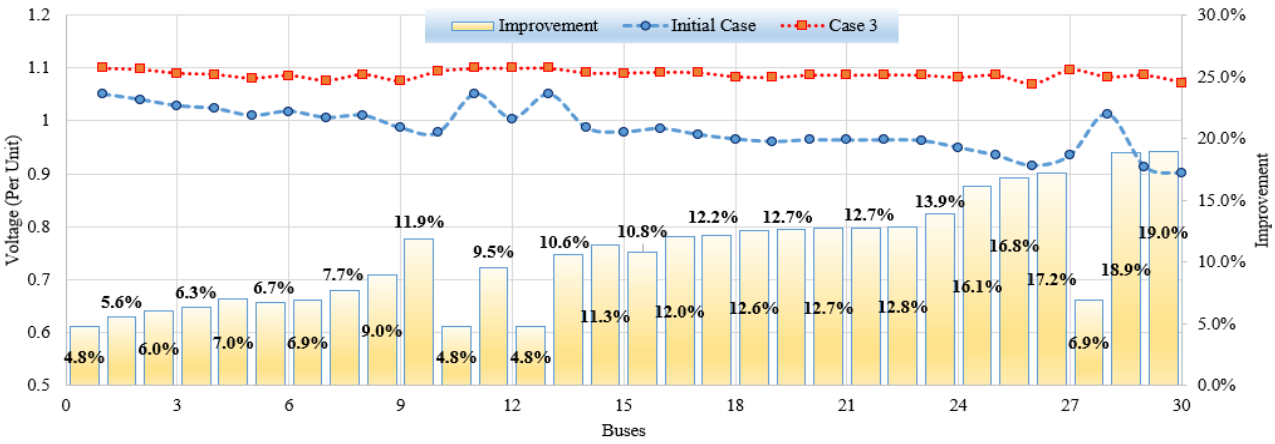

FIGURE 11. Voltage profile and improvements regarding the three TCSC installations (Case 3) against the initial case.

TABLE 8. Statistical analysis of the proposed EGBA with regard to the original GBA and recent approaches for scenario 3.

	AEO	SAO	GWO	AOT	DMO	GBA	EGBA
Best	2.880	2.821	3.187	2.969	3.017	2.7996589	2.7596493
Mean	3.010	2.918	3.468	3.079	3.071	2.8194658	2.7826437
Worst	3.536	3.189	3.856	3.198	3.143	2.8559454	2.816685
STD	0.150	0.123	0.173	0.066	0.029	0.0207062	0.0152856

Besides, Figure 5 displays the convergence curves for the proposed EGBA and the original GBA. The numerical findings unequivocally demonstrate that the proposed EGBA yields considerable economic advantages and outperforms the original GBA in searching. The proposed EGBA converged in less iterations, according to the convergence curves manifested in Figure 5. In order to statistically assess the methodologies that were compared, figure 6 displays the outcomes associated with the proposed EGBA and the original GBA for scenario 1. The corresponding statistical results of the calculated Losses (MW) for this scenario are shown in Table 4. Upon aggregating the lowest indexes from the acquired target values, it is evident that the suggested EGBA offers excellent performance. The original GBA, AEO, SAO, GWO, AOT and DMO get the mean of acquired losses of 2.8331, 3.007, 2.930, 3.472, 3.080, and 3.065 MW, respectively, whereas the mean losses, found in the proposed EGBA, is 2.8092 MW which is lower than the mentioned algorithms. Compared to the outcomes attained by the original GBA, AEO, SAO, GWO, AOT and DMO, the proposed EGBA attains reductions in improvement of the acquired mean of 0.85%, 7.04%, 4.30%, 23.59%, and 9.11%, respectively. According to the worst achieved losses, the proposed EGBA records the lowest losses of 3.038 MW; in contrast, the losses received by GBA, AEO, SAO, GWO, AOT and DMO are 2.8452, 3.180, 3.188, 3.849, 3.172, and 3.109 MW, respectively. The proposed EGBA provides improvement reductions of 1.04%, 12.93%, 13.21%, 36.69%, 12.65% and 10.41%, respectively, compared to the findings obtained by the original GBA, AEO, SAO, GWO, AOT and DMO.

2) SCENARIO 2

The proposed EGBA is used to optimize the allocation of a single TCSC device in order to achieve lowest possible power losses. The acquired outcomes are contrasted with the original GBA, AEO, SAO, GWO, AOT and DMO. In addition to this, Table 5 displays the best control variables, which are the Var source's injection power, the output power and generators' voltage, and the tap value as well as the location and size of the TCSC devices. From this table, the proposed EGBA generates the least amount of power loss of 2.7799 MW. Additionally, the transmission lines (28–27) and (2–5) are chosen by the planned EGBA with compensation values of 49.99% and 25.55 percent subtraction from the installed line reactance.

When comparing the proposed EGBA to the initial scenario, power losses were reduced by 47.66 %. Moreover, the proposed EGBA achieves a noteworthy decrease percentage of 2.12% in the power losses when comparing its results with those of the original GBA. Also, EGBA achieves a decrease percentage of over 3.13% and 1.44 % in comparison to AEO and SAO. In comparison to the GWO, AOT and DMO, the proposed EGBA reduces power losses by 16.08 %, 7.74 %. and 8.14 %, respectively. Besides, Figure 7 displays the convergence curves for the proposed EGBA and the original GBA. The numerical findings unequivocally demonstrate that the proposed EGBA yields considerable economic advantages and outperforms the original GBA in searching. The proposed EGBA converged in less iterations, according to the convergence curves manifested in Figure 7.

In this regard, figure 8 displays the outcomes associated with the proposed EGBA and the original GBA for scenario 2. The corresponding statistical results of the calculated Losses (MW) for this scenario are shown in Table 6. It is clear that the proposed EGBA provides high performance when it aggregates the smallest objective indices. The original GBA, AEO, SAO, GWO, AOT and DMO get the mean of acquired losses of 2.8813, 2.988, 2.938, 3.501, 3.105, and 3.063 MW, respectively, whereas the mean

TABLE 9. Outcomes of the proposed EGBA with respect to the original GBA for TCSC device allocations regarding scenarios 4 and 5.

	Initial scenario	Scenario 4		Scenario 5	
		GBA	EGBA	GBA	EGBA
VG 1	1.05000	1.050721	1.050423	1.099989	1.1
VG 2	1.04000	1.045046	1.041119	1.09738	1.097378
VG 5	1.01000	1.020571	1.017593	1.078957	1.078882
VG 8	1.01000	1.02542	1.019147	1.084472	1.083666
VG 11	1.05000	1.014989	1.015707	1.1	1.1
VG 13	1.05000	1.000265	0.987769	1.1	1.1
Ta 6-9	1.07800	1.035322	1.029245	0.996536	0.994722
Ta 6-10	1.06900	1.043664	1.039036	0.994352	0.994443
Ta 4-12	1.03200	1.038814	1.036882	0.994171	0.992427
Ta 28-27	1.06800	1.041966	1.041278	0.98362	0.987277
Qr 10	0.00000	4.15405	2.00329	4.999738	4.999818
Qr 12	0.00000	3.263136	4.870308	4.998883	4.999991
Qr 15	0.00000	4.995167	3.611414	4.981294	5
Qr 17	0.00000	4.999998	5	4.999933	5
Qr 20	0.00000	4.217359	5	4.172693	4.331609
Qr 21	0.00000	4.990348	4.949422	4.999999	4.99995
Qr 23	0.00000	2.514672	2.075279	2.653166	2.553696
Qr 24	0.00000	5	5	4.999987	4.999983
Qr 29	0.00000	4.00347	4.381049	2.302656	2.496358
PG 1	99.24000	55.91711	66.9805	45.56275	45.5828
PG 2	80.00000	79.97593	80	79.99936	80
PG 5	50.00000	50	50	49.99936	50
PG 8	20.00000	34.99009	34.9641	34.99893	35
PG 11	20.00000	29.99924	29.99998	30	30
PG 13	20.00000	28.92033	17.41212	40	40
First TCSC installed Lines	-	2-5	2-5	6-28	28-27
First TCSC Compensation	-	-49.94%	-49.94%	-49.99%	-50.00%
Second TCSC installed Lines	-	28-27	21-22	9-10	6-28
Second TCSC Compensation	-	-14.18%	50.00%	-50.00%	-50.00%
Third TCSC installed Lines	-	8-28	10-20	24-25	8-28
Third TCSC Compensation	-	-28.87%	-49.99%	50.00%	-45.20%
Losses (MW)	5.832400	3.5973	4.0433	2.8396	2.8172
OSM	26.6334	29.8458	29.9008	29.4808	29.5541

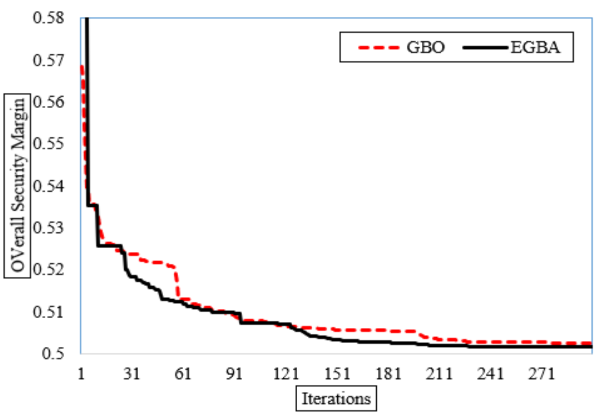

FIGURE 12. Convergence curves for the proposed EGBA versus the original GBA with respect to scenario 4.

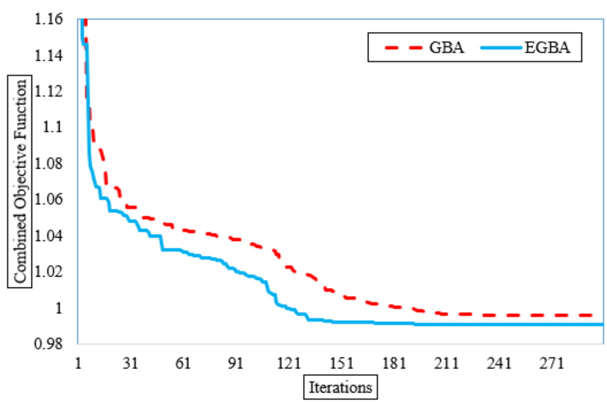

FIGURE 13. Convergence curves for the proposed EGBA versus the original GBA with respect to scenario 5.

losses, found in the proposed EGBA, is 2.7974 MW which is lower than the mentioned algorithms. Compared to the outcomes attained by the original GBA, AEO, SAO, GWO, AOT and DMO, the proposed EGBA attains reductions in improvement of the acquired mean of 3.00%, 6.81%, 5.03%, 25.15%, 11.00%, and 9.49%, respectively. According to the worst achieved losses, the proposed EGBA finds the lowest losses of 2.8234 MW; in contrast, the losses received by GBA, AEO, SAO, GWO, AOT and DMO are 3.1302, 3.214, 3.168, 4.18, 3.181 and 3.119MW, respectively. The proposed EGBA provides improvement reductions of 10.87%, 13.83%, 12.20%, 48.05%, 12.66% and 10.44%, respectively, compared to GBA, AEO, SAO, GWO, AOT and DMO.

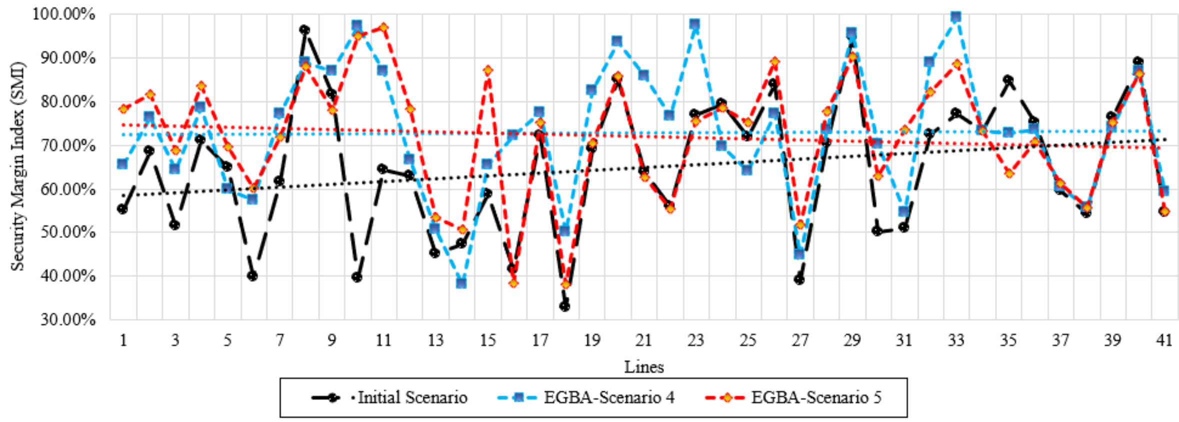

FIGURE 14. **SMI regarding Scenarios 4 and 5 utilizing the proposed EGBA versus the initial scenario.**

TABLE 10. **Outcomes of the proposed EGBA and the original GBA for TCSC device allocations with respect to scenarios 6-8.**

	Initial scenario	Scenario 6		Scenario 7		Scenario 8	
		GBA	EGBA	GBA	EGBA	GBA	EGBA
Vg_{1}	1.010000	1.0988845	1.0999874	1.099977	1.097073	1.00793	1.05166
Vg_{2}	1.010000	1.0934276	1.0941271	1.095513	1.091526	0.99294	1.04443
Vg_{3}	1.010000	1.0963837	1.0968663	1.099981	1.095686	0.99849	1.0466
Vg_{6}	1.010000	1.0998958	1.0980607	1.098768	1.09452	1.01548	1.0499
Vg_{8}	1.010000	1.0986059	1.0982896	1.099603	1.098752	1.03139	1.05302
Vg_{9}	1.010000	1.0816413	1.0806992	1.085981	1.081071	1.00071	1.0309
Vg_{12}	1.010000	1.0890184	1.0862294	1.095583	1.085683	1.00105	1.03672
Tap_{4-18}	0.970000	1.0867576	1.0814775	1.092847	0.96506	1.04246	0.96082
Tap_{4-18}	0.978000	1.0164616	1.0910363	1.052659	1.093106	0.96407	1.01213
Tap_{21-20}	1.043000	1.0124789	1.0483759	1.026323	1.076002	1.03886	1.03236
Tap_{24-25}	1.000000	1.0797724	1.0995063	1.029418	1.078954	1.00294	1.01449
Tap_{24-25}	1.000000	0.9624417	1.0976479	1.044927	1.083855	1.0684	1.04814
Tap_{24-26}	1.043000	1.0122223	1.0804315	0.994227	1.016946	1.01728	0.99308
Tap_{7-29}	0.967000	0.9912568	1.0492207	0.997097	0.991399	0.99398	0.95757
Tap_{34-32}	0.975000	0.9582199	1.0014624	0.985116	0.995503	1.02474	0.94941
Tap_{11-41}	0.955000	1.0999299	0.9015411	0.998072	0.993235	0.96183	0.91439
Tap_{15-45}	0.955000	0.9793998	0.9805513	0.997338	0.981255	0.92501	0.94050
Tap_{14-46}	0.900000	0.9679212	0.9735656	1.002991	0.963666	0.91042	0.94213
Tap_{10-51}	0.930000	0.9732913	0.9826063	1.029773	0.977512	0.96641	0.94056
Tap_{13-49}	0.895000	0.9464282	0.9669984	0.986501	0.953039	0.909519	0.93053
Tap_{11-43}	0.958000	0.9876811	0.9873453	0.986437	1.028425	0.956848	0.936254
Tap_{40-56}	0.958000	1.0864418	0.9697435	0.97277	1.066591	0.980958	1.01481
Tap_{39-57}	0.980000	1.0454983	0.9609632	1.092619	1.05984	0.973298	0.940079
Tap_{9-55}	0.940000	0.980973	1.044776	1.033622	0.98406	1.004027	0.941957
Qc_{18}	10.000000	27.081617	24.711293	18.39356	5.30535	14.91417	11.68338
Qc_{25}	5.900000	14.045868	17.912596	15.13915	17.81111	19.84854	17.22348
Qc_{53}	6.300000	13.394941	11.916993	13.29904	14.77277	14.50879	9.863362
Pg_{1}	478.635000	209.8587460	205.42245180	197.86158	205.577381	193.7548862	202.783103
Pg_{2}	0.000000	2.1806101	0.2893439	9.375461	0.257804	205.5998	197.388
Pg_{3}	40.000000	130.46103	139.09674	135.6695	137.6676	53.09737	13.94101
Pg_{6}	0.000000	99.568362	99.995621	99.13035	99.88743	110.1488	131.4228
Pg_{8}	450.000000	308.14696	305.21702	308.2899	306.5118	47.34087	96.94933
Pg_{9}	0.000000	99.966648	99.999791	99.98456	99.9524	360.6855	312.4387
Pg_{12}	310.000000	409.94388	410	409.9257	410	81.42472	99.45746
First TCSC installed Lines	-	4-18	13-49	13-49	13-49	13-49	13-49
First TCSC Compensation	-	-3.17%	-50.00%	-49.98%	-50.00%	-49.99%	-49.99%
Second TCSC installed Lines	-	-	-	3-4	29-52	4-6	26-27
Second TCSC Compensation	-	-	-	-46.87%	-49.99%	-39.47%	36.54%
Third TCSC installed Lines	-	-	-	-	-	8-9	15-45
Third TCSC Compensation	-	-	-	-	-	-19.86%	36.14%
Losses (MW)	27.835	9.3262325	9.2209663	11.277533	9.0879067	9.1171028	9.0300855

3) SCENARIO 3

In this scenario, the proposed EGBA is used to optimize the allocation of a single TCSC device in order to achieve lowest possible power losses. The acquired outcomes are contrasted with the original GBA, AEO, SAO, GWO, AOT and DMO where Table 7 displays the regarding control variables.

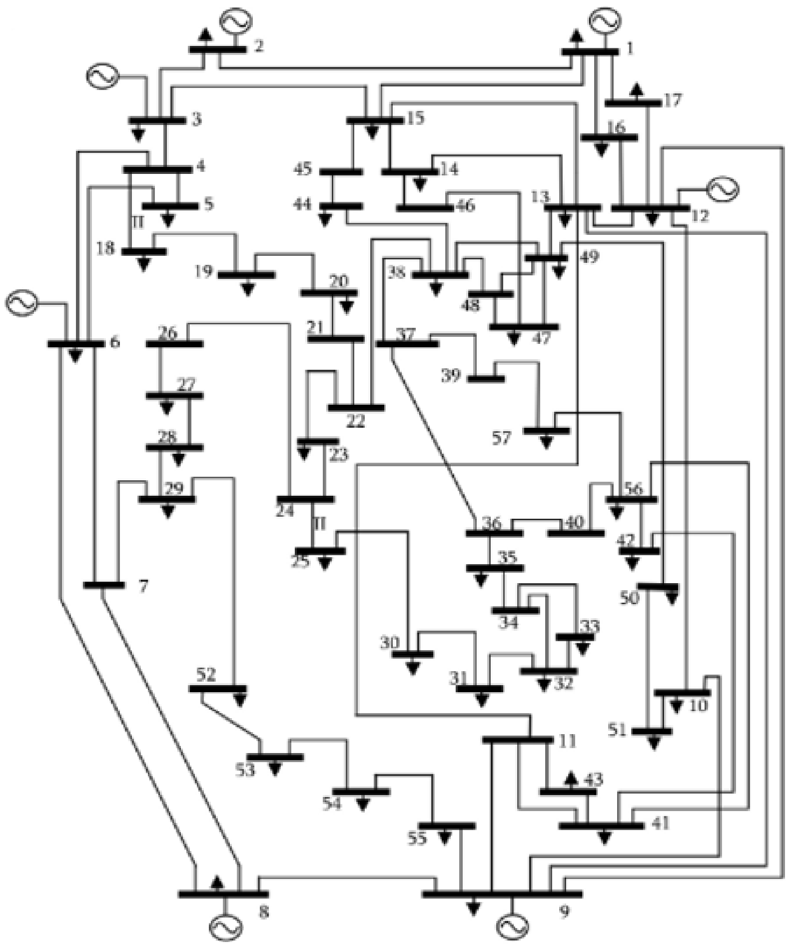

FIGURE 15. Graphic representation for IEEE 57-bus power system [72].

As illustrated from this table, the proposed EGBA generates the least amount of power loss of 2.7596 MW. Additionally, the transmission lines (4-12) and (28-27), and (2–5) are chosen by the planned EGBA with compensation values of 49.8449.99% and −49.9425.55 and −25.20 percent from the installed line reactance, respectively. When comparing the proposed EGBA to the initial scenario, power losses were reduced by 47.32 %. Moreover, the proposed EGBA achieves a noteworthy decrease percentage of 1.45 % in the power losses when comparing its results with those of the original GBA. In addition, the proposed EGBA achieves a decrease percentage of over 4.36% and 2.22% in comparison to the findings achieved by the AEO and SAO. In comparison to the GWO, AOT and DMO, the proposed EGBA reduces power losses by 15.49%, 7.59%. and 9.33%, respectively. Besides, Figure 9 displays the convergence curves for the proposed EGBA and the original GBA. The numerical findings unequivocally demonstrate that the proposed EGBA yields considerable economic advantages and outperforms the original GBA in searching. The proposed EGBA converged in less iterations, according to the convergence curves manifested in Figure 9.

Moreover, figure 10 displays the outcomes associated with the proposed EGBA and the original GBA for scenario 3. The corresponding statistical results of the calculated Losses (MW) for this scenario are shown in Table 8. It is clear that the proposed EGBA provides high performance when it aggregates the fewest objective indices. The original GBA, AEO, SAO, GWO, AOT and DMO get the mean of acquired losses of 2.8194, 3.010, 2.918, 3.468, 3.079, and 3.071 MW, respectively, whereas the mean losses, found in the proposed EGBA, is 2.7826 MW which is lower than the mentioned algorithms. Compared to the outcomes attained by the original GBA, AEO, SAO, GWO, AOT and DMO, the proposed EGBA attains reductions in improvement of the acquired mean of 1.32%, 8.17%, 4.86%, 24.63%, 10.65% and 10.36%, respectively. According to the worst achieved losses, the proposed EGBA finds the lowest losses of 2.8166 MW; in contrast, the losses received by GBA, AEO, SAO, GWO, AOT and DMO are 2.8559, 3.536, 3.189, 3.856, 3.198 and 3.143 MW, respectively. The proposed EGBA provides improvement reductions of 1.39%, 25.54%, 13.22%, 36.90%, 13.54% and 11.59%, respectively, compared to GBA, AEO, SAO, GWO, AOT and DMO.

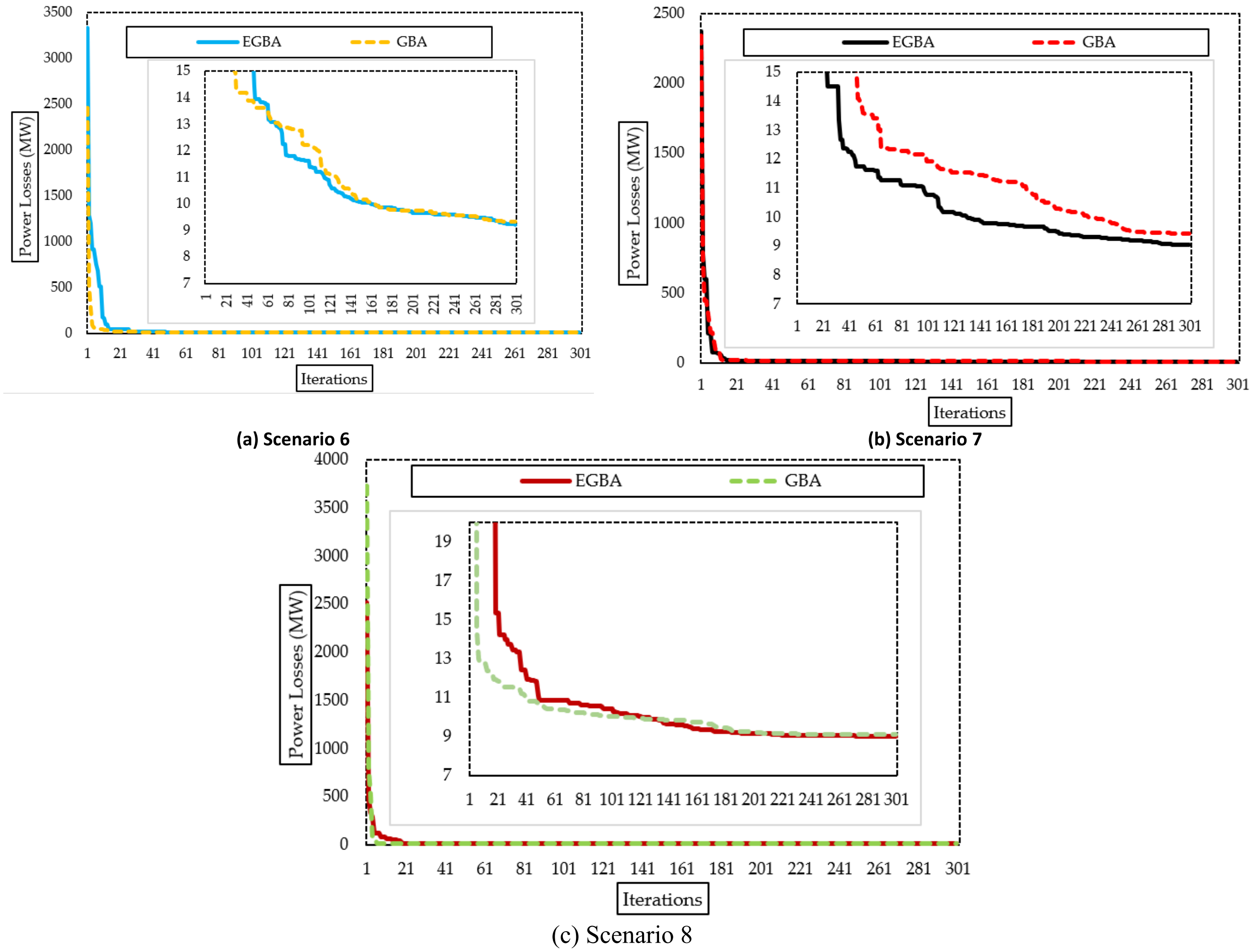

FIGURE 16. Convergence curves for the proposed EGBA versus the original GBA with respect to scenarios 6-8.

The secure operation of the IEEE 30 power networks depends on the entire load buses' voltage profile in comparison to the first scenario, based on the candidate TCSC devices. In this regard, the proposed EGBA is used to compute the voltage magnitude of the buses, and the results are displayed in Figure 11 in comparison to the initial case. Also, the regarding improvement is drawn in the secondary vertical axis.

Looking at the numerical values in this figure, the initial cases range from 0.9012 to 1.05, with an average initial value of approximately 1.00. After the additions of the three TCSC devices, represented by "Case 3," the values generally increase, with the mean value rising to approximately 1.088. This indicates an average improvement of around 8.8% across all cases. While some individual cases show smaller improvements around 4.8%, others demonstrate more substantial enhancements, reaching up to 19.0%. However, the mean improvement of 8.8% suggests that, on average, the additions of the three TCSC devices are effective in positively impacting the outcomes. This analysis underscores the overall effectiveness of the TCSC devices installations based on the proposed EGBA in improving the voltage profile in the system.

C. ENHANCING SECURITY MARGIN ALONGSIDE POWER LOSS MINIMIZATION FOR THE IEEE 30-BUS TRANSMISSION NETWORK

Power system congestion has a substantial impact on the fluctuation of voltage and current, which can cause unintentional variations in the distribution of power throughout the network. A security margin enhancement is required to be included as a critical aim due to this issue. The security margin is a measure of the system's capacity to accept variations in power flow while maintaining safety thresholds [49]. It basically gauges the power system's ability to endure the loss of any part, such a generator or a transmission line, without compromising overall system security. The Security Margin Index (SMI_L) for each individual transmission line

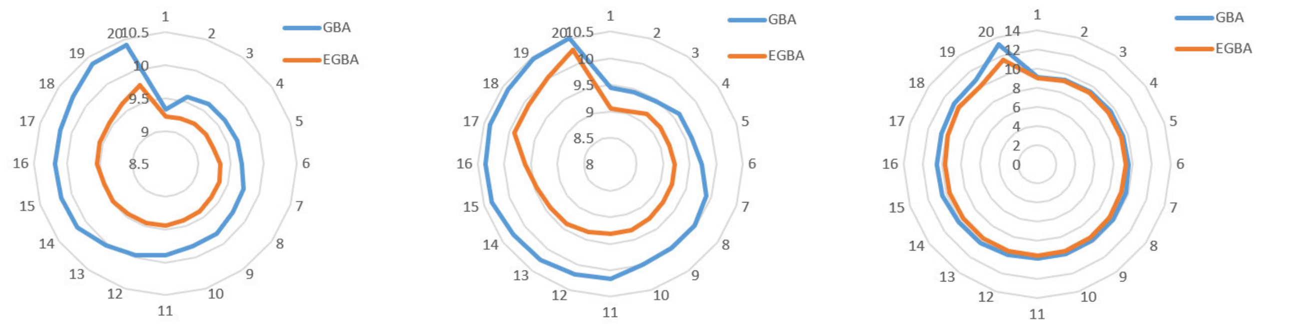

(a) Scenario 6 (b) Scenario 7 (c) Scenario 8

FIGURE 17. Twenty runs for outcomes of proposed EGBA with regard to the original GBA for scenarios 6-8.

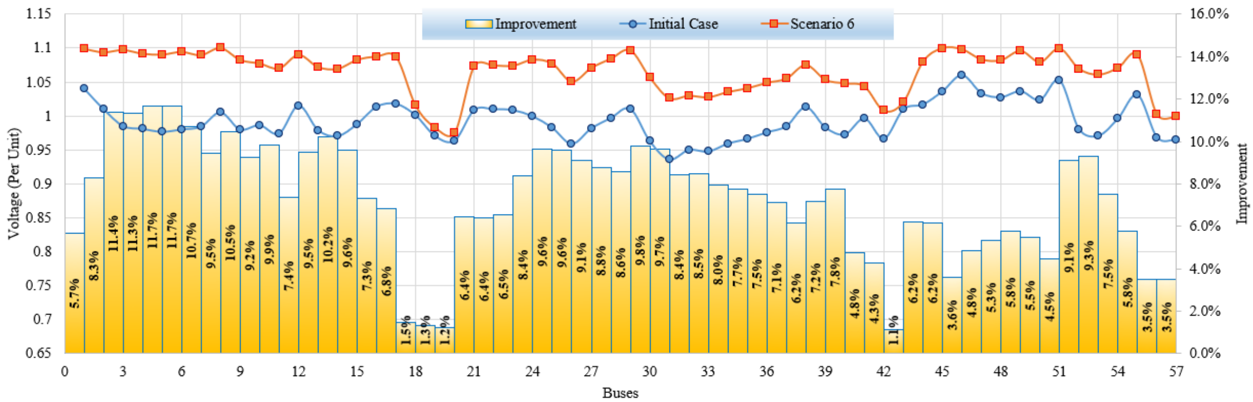

FIGURE 18. Voltage profile and improvements regarding scenario 8 against the initial case.

TABLE 11. Statistical analysis of the proposed EGBA with regard to the original GBA for scenarios 6-8.

	Scenario 6		Scenario 7		Scenario 8	
	GBA	EGBA	GBA	EGBA	GBA	EGBA
Best	9.3262325	9.2209663	11.277533	9.0879067	9.1171028	9.0300855
Mean	9.9099284	9.4209747	10.019497	9.4233737	10.102739	9.6106647
Worst	10.408176	9.7536056	10.494311	10.277184	13.174128	11.535665
STD	0.2968284	0.1413067	0.3623718	0.3430541	0.8766196	0.5398018

(L) can be mathematically modelled as follows [49]:

$$SMI_L = \frac{SF_L^{max} - |SF_L|}{SF_L^{max}}, L = 1, 2, \ldots .N_{lines} \quad (34)$$

where SF_L signifies actual transmission flow and SF_L^{max} is the rated transmission flow constraint in the line (L).

Therefore, the Overall Security Margin (OSM) can be formulated as the summation of the Security Margin Index (SMI_L) of all transmission lines as follows:

$$OSM = \sum_{L=1}^{N_{lines}} SMI_L \quad (35)$$

Based on that, a higher security margin indicates a greater ability of the system to tolerate disturbances and component failures without violating safety constraints. The objective to enhance the security margin involves optimizing the power flow such that the system remains robust against potential disruptions. To optimize the minimization function of power losses and enhance the security margin, the following function is considered:

$$OF = \omega_1 \times \frac{P_{Loss}}{P_{Loss,max}} + \omega_2 \times \frac{OSM_{max}}{OSM} \quad (36)$$

where, ω_1 and ω_2 are the weighting factors while $P_{Loss,max}$ and OSM_{max} are two set values regarding the losses and the overall security margin objectives. This function seeks to minimize the combined objective of the normalized losses and the reciprocal of the security margin. Thus, it maximizes the security margin by minimizing the potential deviations and ensuring the system can handle component losses effectively. Also, the choice of weights reflects the relative significance assigned to each objective, taking into account the trade-offs and priorities among them. Proper

TABLE 12. Outcomes of the proposed EGBA with respect to the original GBA for TCSC device allocations regarding scenarios 9 and 10.

	Initial scenario	Scenario 9		Scenario 10	
		GBA	EGBA	GBA	EGBA
Vg_1	1.010000	1.029205	0.943571	1.008539	1.099776
Vg_2	1.010000	1.029333	0.938509	1.006565	1.0979
Vg_3	1.010000	1.034248	0.940457	1.008744	1.099572
Vg_6	1.010000	1.040398	0.957401	1.016417	1.097693
Vg_8	1.010000	1.044873	0.971959	1.040779	1.099804
Vg_9	1.010000	1.015738	0.933527	1.005245	1.083816
Vg_{12}	1.010000	1.005977	0.926341	0.999101	1.091596
Tap_{4-18}	0.970000	1.084507	0.906135	0.960464	1.076697
Tap_{4-18}	0.978000	0.917781	0.9	1.036283	1.084591
Tap_{21-20}	1.043000	1.090577	0.937057	1.038631	1.096633
Tap_{24-25}	1.000000	0.964875	0.982936	0.916761	1.081158
Tap_{24-25}	1.000000	1.006476	0.944417	1.084537	0.983832
Tap_{24-26}	1.043000	1.016394	1.033951	1.000376	1.059904
Tap_{7-29}	0.967000	1.072402	0.94817	0.995673	1.089494
Tap_{34-32}	0.975000	1.043998	0.913245	1.011484	1.090677
Tap_{11-41}	0.955000	0.978667	0.901292	0.979096	1.045334
Tap_{15-45}	0.955000	1.056802	0.962796	1.053465	1.084978
Tap_{14-46}	0.900000	1.013137	0.926339	1.014787	1.049792
Tap_{10-51}	0.930000	0.99693	0.912064	1.003764	1.081086
Tap_{13-49}	0.895000	0.993682	0.910194	1.025147	1.033916
Tap_{11-43}	0.958000	1.02136	0.943392	1.021054	1.090556
Tap_{40-56}	0.958000	1.012032	1.066108	0.986726	0.98354
Tap_{39-57}	0.980000	0.987046	0.933325	0.957835	1.089799
Tap_{9-55}	0.940000	1.055868	0.920023	1.01081	1.08017
Qc_{18}	10.000000	19.91435	0.44287	23.12521	10.26382
Qc_{25}	5.900000	24.93804	24.11234	27.2582	26.30962
Qc_{53}	6.300000	29.08277	10.93845	1.848242	15.02663
Pg_1	478.635000	102.0447	135.1002	88.35206	129.5019
Pg_2	0.000000	72.83053	33.3253	61.30158	54.08167
Pg_3	40.000000	77.78182	88.42186	98.14144	82.50846
Pg_6	0.000000	90.98896	91.67633	50.21499	64.7072
Pg_8	450.000000	408.4835	412.7616	460.1368	400.8916
Pg_9	0.000000	91.75902	93.58087	84.14613	97.39755
Pg_{12}	310.000000	391.8473	380.0825	392.6954	409.5443
First TCSC installed Lines	-	9-55	24-25	13-49	53-54
First TCSC Compensation	-	-43.91%	-38.42%	-49.22%	-26.20%
Second TCSC installed Lines	-	24-26	14-15	54-55	13-49
Second TCSC Compensation	-	47.76%	-40.41%	-10.10%	-35.58%
Third TCSC installed Lines	-	10-51	3-4	10-51	38-49
Third TCSC Compensation		-47.70%	-2.18%	-29.00%	-48.09%
Losses (MW)	27.835	15.0642	15.8513	15.8116	12.1673
OSM	32.1482	35.5105	37.4007	35.0081	35.4919

weight selection involves understanding the problem domain, stakeholder preferences, and system requirements. To implement this, two different scenarios are addressed. At first (Scenario 4), only the minimization of the normalized reciprocal of the OSM is considered by setting $\omega_1 = 0$ and $\omega_2 = 1$. Second (Scenario 5), both normalized functions are considered of equal importance by setting $\omega_1 = 1$ and $\omega_2 = 1$.

In both scenarios, the proposed EGBA and the original GBA are implemented. Table 9 tabulates their obtained outcomes for TCSC device allocations regarding scenarios 4 and 5 where Figs. 12 and 13 display their convergence properties. As shown, the results demonstrate that the proposed EGBA derives better performance than the GBA. In Scenario 4, the proposed EGBA successfully maximizes the OSM from 26.63 to 29.91 with 10.96% improvement while the GBA increases it to 29.85. Similar results are attained in Scenario 5, the proposed EGBA simultaneously maximizes the OSM and minimizes the power losses to 29.55 and 2.817 MW while the GBA achieves lower OSM of 29.48 and higher losses of 2.84 MW. Alternatively, Fig. 14 illustrates the values of the SMI of each line regarding Scenarios 4 and 5 utilizing the proposed EGBA versus the initial scenario.

As shown, the EGBA provides substantial improvements over the initial scenario. EGBA in both scenarios 4 and 5 demonstrates enhanced performance in the security margin for the IEEE 30-bus transmission network. EGBA-Scenario 4 and EGBA-Scenario 5 show significant improvements over the initial scenario in most instances. For example, the SMI for the first line improves from 55.21% in the initial scenario to 65.52% in EGBA-Scenario 4 and further to 78.43% in EGBA-Scenario 5. This trend is consistent across many

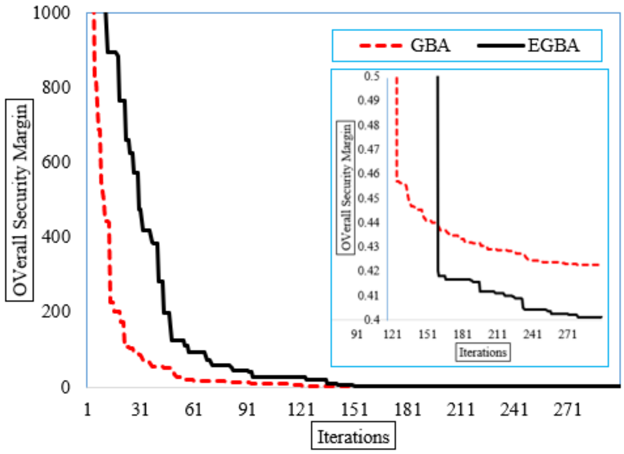

FIGURE 19. Convergence curves for the proposed EGBA versus the original GBA with respect to scenario 9.

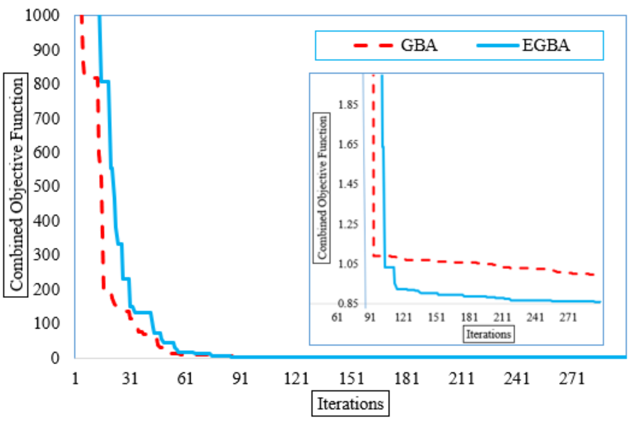

FIGURE 20. Convergence curves for the proposed EGBA versus the original GBA with respect to scenario 10.

lines, indicating that the EGBA algorithm enhancements are effective. These improvements highlight the efficacy of the proposed modifications in optimizing the power system performance.

D. PROPOSED EGBA FOR FIXING TCSC DEVICES IN IEEE 57-BUS TRANSMISSION NETWORK

This part uses the standard IEEE 57-bus transmission network that is shown in Figure 15. There are 57 nodes, 7 generators, 80 lines, 3 capacitive sources on buses, and 17 on-load tap changing transformers in the aforementioned system. The system description is taken from [71]. In order to lower the power losses, the three situations under study are examined with consideration for one, two, and three TCSC devices. Where Table 10 displays their determined control variables, the proposed EGBA and the original GBA are implemented. The results demonstrate that the proposed EGBA reduces power losses by 9.2209663, 9.0879067, and 9.0300855 MW for the scenarios 6-8, while the original GBA reduces power losses by 9.3262325, 11.277533, and 9.1171028 MW, respectively. Alternatively, Fig. 16 indicates the converging features, where iterations to identify and create the best individual are utilized. The numerical findings unequivocally demonstrate that the proposed EGBA yields considerable economic advantages and outperforms the original GBA in searching. The proposed EGBA converged in less iterations, according to the convergence curves manifested in Fig. 16.

To evaluate the overall efficiency of the proposed EGBA in addressing the optimal allocation of TCSC devices in the IEEE 57-bus transmission network, the distribution of the objective function across 20 runs is visually depicted in Figure 17 and summarized in Table 11 for scenarios 6-8. From this data, the following conclusions can be inferred:

- In the sixth scenario, the suggested EGBA yields significant improvements over GBA, with a reduction in the best outcome from 9.326 MW to 9.221 MW, a decrease in mean losses from 9.910 MW to 9.421 MW, and a drop in worst losses from 10.408 MW to 9.754 MW. This indicates improvements of approximately 0.1129%, 5.89%, and 6.68%, respectively, showcasing the EGBA's effectiveness in minimizing losses.
- In the seventh scenario, EGBA demonstrates superiority over GBA across all metrics. It achieves reductions in best, mean, and worst outcomes from 11.278 MW to 9.088 MW, 10.019 MW to 9.423 MW, and 10.494 MW to 10.277 MW, respectively. These improvements correspond to approximately 19.63%, 6.15%, and 2.07%, highlighting the EGBA's consistent ability to optimize TCSC device allocation and reduce losses.
- In the eighth scenario, the proposed EGBA finds the least losses of 9.6106 MW according to the mean acquired losses, whereas the original GBA gets losses of 10.1027 MW.

Overall, the numerical results demonstrate the significant improvements achieved by EGBA over GBA in minimizing losses across different scenarios in the IEEE 57-bus transmission network. The improvements range from approximately 0.11% to 19.63%, underscoring the effectiveness of EGBA in enhancing the allocation of TCSC devices and optimizing power grid performance.

The IEEE 57 power networks' secure operation relies on the voltage profile of all load buses, with the proposed EGBA used to compute bus voltage magnitudes, as shown in Figure 18, illustrating improvements compared to the initial scenario. The initial voltage values range from 0.9359 to 1.0598, averaging around 1.00, while after adding three TCSC devices (Case 3), values generally increase, with the mean rising to approximately 1.0651, indicating an average improvement of about 8.8%. Although some cases show smaller enhancements around 1.1%, others demonstrate more substantial improvements of up to 11.7%. Overall, the mean improvement of 7.22% suggests the effectiveness of TCSC device installations in enhancing the system's voltage profile, as determined by the proposed EGBA.

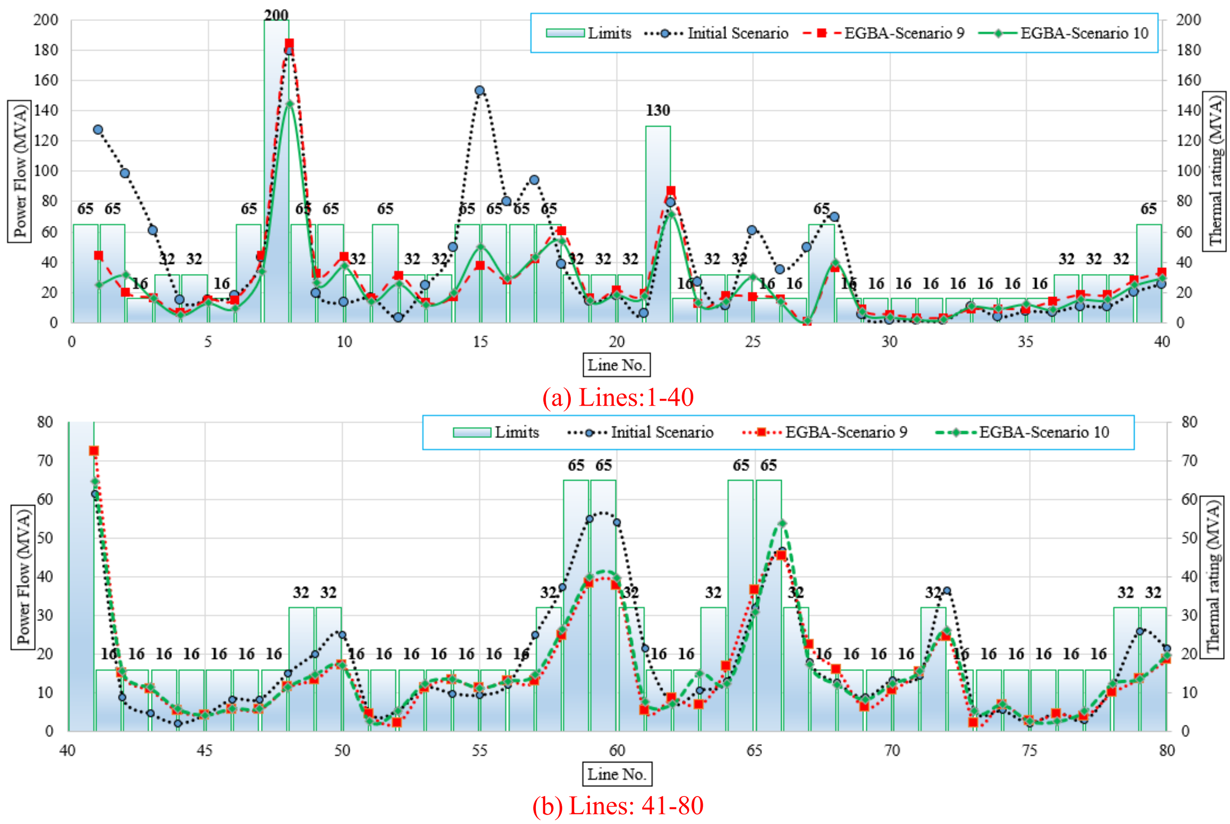

FIGURE 21. MVA thermal limit and flows of each line regarding Scenarios 9 and 10 utilizing the proposed EGBA versus the initial scenario.

In order to address the maximization of the security margin for the IEEE 57-bus system, two different scenarios are addressed. Only the minimization of the normalized reciprocal of the OSM is considered in Scenario 9 while both normalized functions in Eq. (36) are considered of equal importance in Scenario 10.

In both scenarios, the proposed EGBA and the original GBA are implemented. Table 12 tabulates their obtained outcomes for TCSC device allocations regarding scenarios 9 and 10 where Figs. 19 and 20 display their convergence properties. As shown, the results demonstrate that the proposed EGBA derives better performance than the GBA. In Scenario 9, the proposed EGBA successfully maximizes the OSM from 32.15 to 37.4 with 16.33% improvement while the GBA increases it to 35.51 with only 10.45% improvement. Similar results are attained in Scenario 10, the proposed EGBA simultaneously maximizes the OSM and minimizes the power losses to 35.5 and 12.17 MW while the GBA achieves lower OSM of 35 and higher losses of 15.81 MW. Fig. 21 illustrates the thermal limit (MVA) and the power flows of each line regarding Scenarios 9 and 10 utilizing the proposed EGBA versus the initial scenario. As shown, both EGBA-Scenario 9 and Scenario 10 exhibit significant overall improvements in the security margins compared to the initial scenario, indicating the effectiveness of the EGBA in enhancing system security. The EGBA provides significant ability in healing several over loadings in lines numbers (1, 2, 3, 6, 14, 15, 16, 17, 23, 25, 26, 27, 28, 57, 58 and 72) in the initial scenario. EGBA in both scenarios 9 and 10 demonstrates enhanced performance in the security margin for the IEEE 57-bus transmission network.

V. CONCLUSION

This work proposes a novel EGBA to handle two distinct IEEE power systems, with 30 and 57 buses, respectively, and a variety of TCSC devices. These systems are considered to be challenging engineering issues with limited optimal solutions. Important elements of the algorithm, such as the Local Escaping Process (LEP) and Gradient Search Process (GSP), direct the exploration phase and avoid an early convergence to less-than-ideal solutions. Furthermore, a novel feature to the EGBA is the crossover operator which allows TCSC configurations to be exchanged between solutions, and accordingly increasing solution diversity and possibly disclosing new optimal allocations. The applicability of the proposed method is demonstrated by applying it to the CEC 2017 single objective optimisation functions, and its robustness is examined through statistical evaluation and convergence results. Additionally, the proposed EGBA is contrasted with the approaches of AEA, AOT, GTT, RKA, SAO, and SMO. It has been discovered that the proposed EGBA has an exceptional ability to avoid becoming stuck in local optima once it has been implemented on unimodal and multimodal functions. The proposed EGBA is more reliable in reaching the optimum values over several runs, according to the statistical analysis of the benchmark functions. The proposed EGBA effectively reduces power losses compared to several techniques. It also converges faster than the original GBA in reducing power losses. Besides minimizing losses, the EGBA aims to enhance the security margin of transmission lines to optimize power flow. For the IEEE 30 bus system, the EGBA increased the OSM with a 10.96% improvement while it raised the OSM with a 16.33% improvement for the IEEE 57 bus system. Additionally, the EGBA significantly mitigates several line overloads.

ACKNOWLEDGMENT

The authors extend their appreciation to Prince Sattam bin Abdulaziz University for funding this research work through the project number (PSAU/2024/01/29312).

REFERENCES

[1] J. A. Momoh, R. Adapa, and M. E. El-Hawary, "A review of selected optimal power flow literature to 1993. I. nonlinear and quadratic programming approaches," *IEEE Trans. Power Syst.*, vol. 14, no. 1, pp. 96–104, Feb. 1993, doi: 10.1109/59.744492.

[2] I. A. Ibrahim and M. J. Hossain, "Low voltage distribution networks modeling and unbalanced (optimal) power flow: A comprehensive review," *IEEE Access*, vol. 9, pp. 143026–143084, 2021, doi: 10.1109/ACCESS.2021.3120803.

[3] A. Alhejji, M. Ebeed Hussein, S. Kamel, and S. Alyami, "Optimal power flow solution with an embedded center-node unified power flow controller using an adaptive grasshopper optimization algorithm," *IEEE Access*, vol. 8, pp. 119020–119037, 2020, doi: 10.1109/ACCESS.2020.2993762.

[4] S. Dash, K. R. Subhashini, and J. Satapathy, "Efficient utilization of power system network through optimal location of FACTS devices using a proposed hybrid meta-heuristic ant lion-moth flame-salp swarm optimization algorithm," *Int. Trans. Electr. Energy Syst.*, vol. 30, no. 7, Jul. 2020, doi: 10.1002/2050-7038.12402.

[5] A. Vaccaro and C. A. Cañizares, "A knowledge-based framework for power flow and optimal power flow analyses," *IEEE Trans. Smart Grid*, vol. 9, no. 1, pp. 230–239, Jan. 2018, doi: 10.1109/TSG.2016.2549560.

[6] J. Singh, N. K. Yadav, and S. K. Gupta, "Enhancement of available transfer capability using TCSC with hybridized model: Combining lion and moth flame algorithms," *Concurrency Computation: Pract. Exper.*, vol. 34, no. 21, p. e7052, Sep. 2022, doi: 10.1002/cpe.7052.

[7] S. B. Pandya, S. Ravichandran, P. Manoharan, P. Jangir, and H. H. Alhelou, "Multi-objective optimization framework for optimal power flow problem of hybrid power systems considering security constraints," *IEEE Access*, vol. 10, pp. 103509–103528, 2022, doi: 10.1109/ACCESS.2022.3209996.

[8] T. Ding, R. Bo, Z. Bie, and X. Wang, "Optimal selection of phase shifting transformer adjustment in optimal power flow," *IEEE Trans. Power Syst.*, vol. 32, no. 3, pp. 2464–2465, May 2017, doi: 10.1109/TPWRS.2016.2600098.

[9] R. Devarapalli, B. Bhattacharyya, and N. K. Sinha, "An intelligent EGWO-SCA-CS algorithm for PSS parameter tuning under system uncertainties," *Int. J. Intell. Syst.*, vol. 35, no. 10, pp. 1520–1569, Oct. 2020, doi: 10.1002/int.22263.

[10] R. M. Mathur and R. K. Varma, *Thyristor-based Facts Controllers for Electrical Transmission Systems*. Wiley, 2002, doi: 10.1109/9780470546680.

[11] C. Rehtanz, *Flexible AC Transmission Systems: Modelling & Control* (Power systems). Springer, 2006, doi: 10.1007/3-540-30607-2.

[12] J. Morsali, K. Zare, and M. Tarafdar Hagh, "Performance comparison of TCSC with TCPS and SSSC controllers in AGC of realistic interconnected multi-source power system," *Ain Shams Eng. J.*, vol. 7, no. 1, pp. 143–158, Mar. 2016, doi: 10.1016/j.asej.2015.11.012.

[13] A. M. Shaheen, R. A. El-Sehiemy, and S. M. Farrag, "Optimal reactive power dispatch using backtracking search algorithm," *Austral. J. Electr. Electron. Eng.*, vol. 13, no. 3, pp. 200–210, Jul. 2016, doi: 10.1080/1448837x.2017.1325134.

[14] M. Usman and F. Capitanescu, "A novel tractable methodology to stochastic multi-period AC OPF in active distribution systems using sequential linearization algorithm," *IEEE Trans. Power Syst.*, vol. 38, pp. 1–15, 2023, doi: 10.1109/TPWRS.2022.3197884.

[15] A. A. Sousa, G. L. Torres, and C. A. Cañizares, "Robust optimal power flow solution using trust region and interior-point methods," *IEEE Trans. Power Syst.*, vol. 26, no. 2, pp. 487–499, May 2011, doi: 10.1109/TPWRS.2010.2068568.

[16] R. A. El Sehiemy, A. A. Abou El Ela, and A. Shaheen, "A multi-objective fuzzy-based procedure for reactive power-based preventive emergency strategy," *Int. J. Eng. Res. Afr.*, vol. 13, pp. 91–102, Dec. 2014, doi: 10.4028/www.scientific.net/jera.13.91.

[17] O. Crisan and M. A. Mohtadi, "Efficient identification of binding inequality constraints in the optimal power flow Newton approach," *IEE Proc. C Gener., Transmiss. Distribution*, vol. 139, no. 5, p. 365, 1992, doi: 10.1049/ip-c.1992.0053.

[18] H. Dommel and W. Tinney, "Optimal power flow solutions," *IEEE Trans. Power App. Syst.*, vol. PAS-87, no. 10, pp. 1866–1876, Oct. 1968, doi: 10.1109/TPAS.1968.292150.

[19] A. Santos and G. R. M. da Costa, "Optimal-power-flow solution by Newton's method applied to an augmented Lagrangian function," *IEE Proc. Gener., Transmiss. Distribution*, vol. 142, no. 1, p. 33, Jan. 1995, doi: 10.1049/ip-gtd:19951586.

[20] Z. Ullah, "A mini-review: Conventional and metaheuristic optimization methods for the solution of optimal power flow (OPF) problem," in *Advances in Intelligent Systems and Computing*, vol. 1151. Springer, 2020, doi: 10.1007/978-3-030-44041-1_29.

[21] A. E. Chaib, H. R. E. H. Bouchekara, R. Mehasni, and M. A. Abido, "Optimal power flow with emission and non-smooth cost functions using backtracking search optimization algorithm," *Int. J. Electr. Power Energy Syst.*, vol. 81, pp. 64–77, Oct. 2016, doi: 10.1016/j.ijepes.2016.02.004.

[22] S. S. Reddy and P. R. Bijwe, "Efficiency improvements in meta-heuristic algorithms to solve the optimal power flow problem," *Int. J. Emerg. Electric Power Syst.*, vol. 17, no. 6, pp. 631–647, Dec. 2016, doi: 10.1515/ijeeps-2015-0216.

[23] T. T. Nguyen, "A high performance social spider optimization algorithm for optimal power flow solution with single objective optimization," *Energy*, vol. 171, pp. 218–240, Mar. 2019, doi: 10.1016/j.energy.2019.01.021.

[24] E. E. Elattar and S. K. ElSayed, "Modified Jaya algorithm for optimal power flow incorporating renewable energy sources considering the cost, emission, power loss and voltage profile improvement," *Energy*, vol. 178, pp. 598–609, Jul. 2019, doi: 10.1016/j.energy.2019.04.159.

[25] S. R. Nayak, R. K. Khadanga, D. Das, Y. Arya, S. Panda, and P. R. Sahu, "Influence of ultracapacitor and plug-in electric vehicle for frequency regulation of hybrid power system utilizing artificial gorilla troops optimizer algorithm," *Int. J. Energy Res.*, vol. 2023, pp. 1–18, Nov. 2023, doi: 10.1155/2023/6689709.

[26] M. Mojtahedzadeh Larijani, M. Ahmadi Kamarposhti, and T. Nouri, "Stochastic unit commitment study in a power system with flexible load in presence of high penetration renewable farms," *Int. J. Energy Res.*, vol. 2023, pp. 1–19, Jul. 2023, doi: 10.1155/2023/9979610.

[27] K. Świrydowicz, N. Koukpaizan, T. Ribizel, F. Göbel, S. Abhyankar, H. Anzt, and S. Peleš, "GPU-resident sparse direct linear solvers for alternating current optimal power flow analysis," *Int. J. Electr. Power Energy Syst.*, vol. 155, Jan. 2024, Art. no. 109517, doi: 10.1016/j.ijepes.2023.109517.

[28] M. Kaur and N. Narang, "An integrated optimization technique for optimal power flow solution," *Soft Comput.*, vol. 24, no. 14, pp. 10865–10882, Jul. 2020, doi: 10.1007/s00500-019-04590-3.

[29] A. M. Shaheen, R. A. El-Sehiemy, E. E. Elattar, and A. S. Abd-Elrazek, "A modified crow search optimizer for solving non-linear OPF problem with emissions," *IEEE Access*, vol. 9, pp. 43107–43120, 2021, doi: 10.1109/ACCESS.2021.3060710.

[30] V. S. Rao, M. Ravindra, A. S. Veerendra, R. S. Rao, A. Ramesh, and K. M. K. Reddy, "Sensitivity based allocation of FACTS devices in a transmission system considering differential analysis," in *Proc. Int. Conf. Artif. Intell. Techn. Elect. Eng. Syst.*, 2023, pp. 48–60.

[31] A. Adhikari, F. Jurado, S. Naetiladdanon, A. Sangswang, S. Kamel, and M. Ebeed, "Stochastic optimal power flow analysis of power system with renewable energy sources using adaptive lightning attachment procedure optimizer," *Int. J. Electr. Power Energy Syst.*, vol. 153, Nov. 2023, Art. no. 109314, doi: 10.1016/j.ijepes.2023.109314.

[32] A. Nerger, A. C. P. Martins, E. M. Soler, A. R. Balbo, and L. Nepomuceno, "A nonlinear multi-period hydrothermal optimal power flow model for hydropower systems," *Int. J. Electr. Power Energy Syst.*, vol. 155, Jan. 2024, Art. no. 109585, doi: 10.1016/j.ijepes.2023.109585.

[33] Z. Fan, Z. Yang, and J. Yu, "Error bound of convex approximation for optimal power flow model: A general solving approach based on optimality gap," *Int. J. Electr. Power Energy Syst.*, vol. 157, Jun. 2024, Art. no. 109884, doi: 10.1016/j.ijepes.2024.109884.

[34] A. M. Shaheen, R. A. El-Sehiemy, H. M. Hasanien, and A. Ginidi, "An enhanced optimizer of social network search for multi-dimension optimal power flow in electrical power grids," *Int. J. Electr. Power Energy Syst.*, vol. 155, Jan. 2024, Art. no. 109572, doi: 10.1016/j.ijepes.2023.109572.

[35] A. Shaheen, A. Ginidi, R. El-Sehiemy, A. Elsayed, E. Elattar, and H. T. Dorrah, "Developed gorilla troops technique for optimal power flow problem in electrical power systems," *Mathematics*, vol. 10, no. 10, p. 1636, May 2022, doi: 10.3390/math10101636.

[36] A. Ginidi, E. Elattar, A. Shaheen, A. Elsayed, R. El-Sehiemy, and H. Dorrah, "Optimal power flow incorporating thyristor-controlled series capacitors using the gorilla troops algorithm," *Int. Trans. Electr. Energy Syst.*, vol. 2022, pp. 1–23, Aug. 2022, doi: 10.1155/2022/9448199.

[37] W. Liu, X. Yang, T. Zhang, and A. Abu-Siada, "Multi-objective optimal allocation of TCSC for power systems with wind power considering load randomness," *J. Electr. Eng. Technol.*, vol. 18, no. 2, pp. 765–777, Mar. 2023, doi: 10.1007/s42835-022-01233-w.

[38] N. K. Yadav, "Optimizing TCSC configuration via genetic algorithm for ATC enhancement," *Multimedia Tools Appl.*, vol. 82, no. 25, pp. 38715–38741, Oct. 2023, doi: 10.1007/s11042-023-15043-3.

[39] G. Moustafa, M. A. Tolba, A. M. El-Rifaie, A. Ginidi, A. M. Shaheen, and S. Abid, "A subtraction-average-based optimizer for solving engineering problems with applications on TCSC allocation in power systems," *Biomimetics*, vol. 8, no. 4, p. 332, Jul. 2023, doi: 10.3390/biomimetics8040332.

[40] D. Prasad and V. Mukherjee, "A novel symbiotic organisms search algorithm for optimal power flow of power system with FACTS devices," *Eng. Sci. Technol., Int. J.*, vol. 19, no. 1, pp. 79–89, Mar. 2016, doi: 10.1016/j.jestch.2015.06.005.

[41] R. P. Singh, V. Mukherjee, and S. P. Ghoshal, "Particle swarm optimization with an aging leader and challengers algorithm for optimal power flow problem with FACTS devices," *Int. J. Electr. Power Energy Syst.*, vol. 64, pp. 1185–1196, Jan. 2015, doi: 10.1016/j.ijepes.2014.09.005.

[42] M. Balasubbareddy, D. Dwivedi, G. V. K. Murthy, and K. S. Kumar, "Optimal power flow solution with current injection model of generalized interline power flow controller using ameliorated ant lion optimization," *Int. J. Electr. Comput. Eng. (IJECE)*, vol. 13, no. 1, p. 1060, Feb. 2023, doi: 10.11591/ijece.v13i1.pp1060-1077.

[43] M. B. Shafik, H. Chen, G. I. Rashed, and R. A. El-Sehiemy, "Adaptive multi objective parallel seeker optimization algorithm for incorporating TCSC devices into optimal power flow framework," *IEEE Access*, vol. 7, pp. 36934–36947, 2019, doi: 10.1109/ACCESS.2019.2905266.

[44] D. K. Molzahn, F. Dörfler, H. Sandberg, S. H. Low, S. Chakrabarti, R. Baldick, and J. Lavaei, "A survey of distributed optimization and control algorithms for electric power systems," *IEEE Trans. Smart Grid*, vol. 8, no. 6, pp. 2941–2962, Nov. 2017, doi: 10.1109/TSG.2017.2720471.

[45] A. Narain, S. K. Srivastava, and S. N. Singh, "A novel sensitive based approach to ATC enhancement in wind power integrated transmission system," *Social Netw. Appl. Sci.*, vol. 3, no. 5, May 2021, Art. no. 563, doi: 10.1007/s42452-021-04559-8.

[46] A. Sahoo, P. K. Hota, P. R. Sahu, F. Alsaif, S. Alsulamy, and T. S. Ustun, "Optimal congestion management with FACTS devices for optimal power dispatch in the deregulated electricity market," *Axioms*, vol. 12, no. 7, p. 614, Jun. 2023, doi: 10.3390/axioms12070614.

[47] N. Avudayappan and S. N. Deepa, "Congestion management in deregulated power system using hybrid cat-firefly algorithm with TCSC and SVC FACTS devices," *COMPEL Int. J. Comput. Math. Electr. Electron. Eng.*, vol. 35, no. 5, pp. 1524–1537, Sep. 2016, doi: 10.1108/compel-11-2015-0423.

[48] M. Gupta, V. Kumar, G. K. Banerjee, and N. K. Sharma, "Mitigating congestion in a power system and role of FACTS devices," *Adv. Electr. Eng.*, vol. 2017, pp. 1–7, Jan. 2017, doi: 10.1155/2017/4862428.

[49] A. Gautam, Ibraheem, G. Sharma, M. Kumawat, and M. F. Ahmer, "A novel solution for the power transmission congestion of deregulated power system using TCSC and TLBO algorithm," *e-Prime Adv. Electr. Eng., Electron. Energy*, vol. 8, Jun. 2024, Art. no. 100592, doi: 10.1016/j.prime.2024.100592.

[50] M. Ebeed, A. Mostafa, M. M. Aly, F. Jurado, and S. Kamel, "Stochastic optimal power flow analysis of power systems with wind/PV/ TCSC using a developed Runge Kutta optimizer," *Int. J. Electr. Power Energy Syst.*, vol. 152, Oct. 2023, Art. no. 109250, doi: 10.1016/j.ijepes.2023.109250.

[51] D. Lu, *An Update on Power Quality*. Intech, 2013, doi: 10.5772/51135.

[52] K. K. Sen and M. L. Sen, *Introduction to FACTS Controllers: Theory, Modeling, and Applications*. Wiley, 2009, doi: 10.1002/9780470524756.

[53] C. Gupta, "Book review: FACTS: Modelling and simulation in power networks," *Int. J. Electr. Eng. Educ.*, vol. 42, no. 2, pp. 209–210, Apr. 2005, doi: 10.7227/ijeee.42.2.8.

[54] H. Bakır, "Dynamic fitness-distance balance-based artificial rabbits optimization algorithm to solve optimal power flow problem," *Expert Syst. Appl.*, vol. 240, Apr. 2024, Art. no. 122460, doi: 10.1016/j.eswa.2023.122460.

[55] S. Sarhan, A. Shaheen, R. El-Sehiemy, and M. Gafar, "Optimal multi-dimension operation in power systems by an improved artificial hummingbird optimizer," *Human-Centric Comput. Inf. Sci.*, vol. 13, pp. 1–27, Apr. 2023, doi: 10.22967/HCIS.2023.13.013.

[56] J. Zhang, J. Cai, S. Wang, and P. Li, "Many-objective optimal power flow problems based on distributed power flow calculations for hierarchical partition-managed power systems," *Int. J. Electr. Power Energy Syst.*, vol. 148, Jun. 2023, Art. no. 108945, doi: 10.1016/j.ijepes.2023.108945.

[57] I. Ahmadianfar, O. Bozorg-Haddad, and X. Chu, "Gradient-based optimizer: A new metaheuristic optimization algorithm," *Inf. Sci.*, vol. 540, pp. 131–159, Nov. 2020, doi: 10.1016/j.ins.2020.06.037.

[58] M. S. Daoud, M. Shehab, H. M. Al-Mimi, L. Abualigah, R. A. Zitar, and M. K. Y. Shambour, "Gradient-based optimizer (GBO): A review, theory, variants, and applications," *Arch. Comput. Methods Eng.*, vol. 30, no. 4, pp. 2431–2449, May 2023, doi: 10.1007/s11831-022-09872-y.

[59] M.-S. C. R. D. Zimmerman. *Matpower [Software]*. Accessed: Dec. 16, 2016. [Online]. Available: https://matpower.org

[60] Y. Shen, Z. Liang, H. Kang, X. Sun, and Q. Chen, "A modified jSO algorithm for solving constrained engineering problems," *Symmetry*, vol. 13, no. 1, p. 63, Dec. 2020, doi: 10.3390/sym13010063.

[61] L. Abualigah, D. Yousri, M. Abd Elaziz, A. A. Ewees, M. A. A. Al-qaness, and A. H. Gandomi, "Aquila optimizer: A novel meta-heuristic optimization algorithm," *Comput. Ind. Eng.*, vol. 157, Jul. 2021, Art. no. 107250, doi: 10.1016/j.cie.2021.107250.

[62] A. Shaheen, R. El-Sehiemy, A. El-Fergany, and A. Ginidi, "Fuel-cell parameter estimation based on improved gorilla troops technique," *Sci. Rep.*, vol. 13, no. 1, p. 8685, May 2023, doi: 10.1038/s41598-023-35581-y.

[63] J. Raeisi-Gahruei and Z. Beheshti, "The electricity consumption prediction using hybrid red kite optimization algorithm with multi-layer perceptron neural network," *J. Intell. Proced. Electr. Technol.*, vol. 15, no. 60, pp. 19–40, 2022.

[64] P. Trojovský and M. Dehghani, "Subtraction-average-based optimizer: A new swarm-inspired metaheuristic algorithm for solving optimization problems," *Biomimetics*, vol. 8, no. 2, p. 149, Apr. 2023, doi: 10.3390/biomimetics8020149.

[65] S. Li, H. Chen, M. Wang, A. A. Heidari, and S. Mirjalili, "Slime mould algorithm: A new method for stochastic optimization," *Future Gener. Comput. Syst.*, vol. 111, pp. 300–323, Oct. 2020, doi: 10.1016/j.future.2020.03.055.

[66] J. O. Agushaka, A. E. Ezugwu, and L. Abualigah, "Dwarf mongoose optimization algorithm," *Comput. Methods Appl. Mech. Eng.*, vol. 391, Mar. 2022, Art. no. 114570, doi: 10.1016/j.cma.2022.114570.

[67] B. Abdollahzadeh, F. S. Gharehchopogh, and S. Mirjalili, "Artificial gorilla troops optimizer: A new nature-inspired metaheuristic algorithm for global optimization problems," *Int. J. Intell. Syst.*, vol. 36, no. 10, pp. 5887–5958, Jul. 2021, doi: 10.1002/int.22535.

[68] A. M. Shaheen, R. A. El-Sehiemy, M. M. Alharthi, S. S. M. Ghoneim, and A. R. Ginidi, "Multi-objective jellyfish search optimizer for efficient power system operation based on multi-dimensional OPF framework," *Energy*, vol. 237, Dec. 2021, Art. no. 121478, doi: 10.1016/j.energy.2021.121478.

[69] M. Ghasemi, M. Taghizadeh, S. Ghavidel, J. Aghaei, and A. Abbasian, "Solving optimal reactive power dispatch problem using a novel teaching–learning-based optimization algorithm," *Eng. Appl. Artif. Intell.*, vol. 39, pp. 100–108, Mar. 2015, doi: 10.1016/j.engappai.2014.12.001.

[70] S. Sarhan, A. Shaheen, R. El-Sehiemy, and M. Gafar, "An augmented social network search algorithm for optimal reactive power dispatch problem," *Mathematics*, vol. 11, no. 5, p. 1236, Mar. 2023, doi: 10.3390/math11051236.

[71] A. Shabanpour-Haghighi, A. R. Seifi, and T. Niknam, ''A modified teaching–learning based optimization for multi-objective optimal power flow problem,'' *Energy Convers. Manage.*, vol. 77, pp. 597–607, Jan. 2014, doi: 10.1016/j.enconman.2013.09.028.
[72] A. M. Shaheen, R. A. El-Sehiemy, A. M. Elsayed, and E. E. Elattar, ''Multi-objective manta ray foraging algorithm for efficient operation of hybrid AC/DC power grids with emission minimisation,'' *IET Gener., Transmiss. Distribution*, vol. 15, no. 8, pp. 1314–1336, Apr. 2021, doi: 10.1049/gtd2.12104.

ALI S. ALJUMAH was born in July 1989. He received the B.Sc. degree in electrical engineering from the King Fahd University of Petroleum and Minerals (KFUPM), Saudi Arabia, in 2012, and the M.Sc. degree and the Ph.D. degree in electrical engineering from the University of South Florida (USF), USA, in 2016 and 2022, respectively.

Currently, he works as an Assistant Professor with the Electrical Engineering Department, Prince Sattam Bin Abdulaziz University. His research interests include power systems modeling, stability, and renewable energy sources integration to a power grid.

MOHAMMED H. ALQAHTANI (Member, IEEE) was born in October 1989. He received the B.S. degree in electrical engineering from Prince Sattam Bin Abdulaziz University, Saudi Arabia, in 2012, the M.S. degree from the University of South Florida (USF), in 2016, and the Ph.D. degree from the USF Smart Grid Power Systems Laboratory, in 2021. He is currently an Assistant Professor with Prince Sattam Bin Abdulaziz University. His research interests include power system computing and modeling.

ABDULLAH M. SHAHEEN was born in Tanta, Egypt, in 1985. He received the B.Sc. degree from Suez Canal University, Port Said, Egypt, in 2007, and the M.Sc. and Ph.D. degrees from Menoufia University, Shebeen El-Kom, Egypt, in 2012 and 2016, respectively. He is currently with the Department of Electrical Engineering, Faculty of Engineering, Suez University, El Suweis, Egypt. His research interests include power system operation, control, and planning, the applications of optimization algorithms in electric power systems, renewable integration, and smart grid.

ABDALLAH M. ELSAYED was born in Damietta, Egypt, in 1986. He received the B.Sc., M.Sc., and Ph.D. degrees from Menoufia University, Shebeen El-Kom, Egypt, in 2008, 2012, and 2016, respectively. He is currently a Lecturer with the Department of Electrical Engineering, Faculty of Engineering, Damietta University, New Damietta, Egypt. His research interests include power system operation, control, and planning, applications of modern optimization techniques for variant electric power systems applications, renewable sources, and smart grids.